Physical Model for Cell Selectivity of Antimicrobial Peptides

by

Azadeh Bagheri

A thesis
presented to the University of Waterloo
in fulfillment of the
thesis requirement for the degree of
Master of Science
in
Physics

Waterloo, Ontario, Canada, 2013

I hereby declare that I am the sole author of this thesis. This is a true copy of the thesis, including any required final revisions, as accepted by my examiners.

I understand that my thesis may be made electronically available to the public.

Abstract

Antimicrobial peptides (AMPs) are relatively-short chain molecules that living organisms use to defend themselves against a wide range of invading microorganisms such as bacteria and viruses. They selectively bind to and kill microbes over host cells by permeabilizing cell membranes or by inhibiting the biological functions of intra-cellular components. Despite its significance in determining their cell selectivity, however, the cell-concentration dependence of AMP's membrane-perturbing activity has not been criticality examined.

In this thesis, we present a physical model for cell selectivity of AMPs, especially its cell-concentration dependence. To this end, we use a coarse-grained model that captures essential molecular details such as lipid composition (*e.g.,* fraction of anionic lipids) and peptide amphiphilicity and charge. In particular, we calculate the surface coverage of peptides in the membrane-perturbing mode as a function of peptide and cell densities: those that bind to the interface between lipid headgroups and tails. This allows us to extract the minimum inhibitory concentration (MIC) and the minimum hemolytic concentration (MHC) of the peptides. Our results show that both MIC and MHC increase as the cell density increases so that the peptide selectivity (given by MHC/MIC) decreases with increasing cell density. Our results will help resolve conflicting interpretations of peptide-selectivity experiments.

Acknowledgements

I would like to express my sincere gratitude to my supervisor, Dr. Bae-Yeun Ha, for the useful comments, remarks and engagement through the learning process of this thesis. I am grateful to my defence and advisory committee members, Dr. Russell Thompson, Dr. Zoya Leonenko, and Dr. Mohammad Kohandel, for their constructive comments and suggestions that I found useful in improving this work. I am also thankful to Sattar Taheri-Araghi and Zheng Ma, the senior members of our research group. Their constructive pieces of advice and cooperation helped me a lot to progress in my research projects.

I am particularly thankful to my parents for everything I have earned in my life. Their unconditional love and support have always encouraged me to pursue my dreams and never give up. My sisters deserve my wholehearted thanks as well.

My special thanks go to my amazing friends Kier von Konigslow and Rabab Mashayekhi for all their support and encouragement in my many, many moments of crisis.

This thesis is dedicated to my parents
for all they did.

Table of Contents

List of Figures

Chapter 1

Introduction

1.1 Motivation and goals

During the last couple of decades, there has been a noticeable rise in bacterial resistance. As a result, many antibiotics have become ineffective against an increasing number of pathogenic microbes. Accordingly, much effort has been made to develop new antimicrobial therapeutics. Antimicrobial peptides (AMPs) or their analogues have been considered as promising candidates among others [2].

AMPs are key components of the innate immune system of almost all living organisms from prokaryotes to humans [3]. While AMPs have constantly provided a first-line of defence for the organisms against microbes and other invading pathogens, microbes have not easily adapted to evade their lethal mechanism of action. In other words, AMP's mechanism of action does not easily induce microbial resistance. Furthermore, these peptides have a broad-spectrum antimicrobial activity. They have been shown to be active against a wide range of bacteria, fungi, yeast, viruses, and even tumor cells. As a result, AMPs are believed to have a great potential to solve the bacterial resistance problem, as they present a novel class of antibiotics.

The antimicrobial or host defence peptides have stimulated considerable research not only to understand the biology of the innate immune system, but also to design new

therapeutic compounds [2, 4]. To date, a few AMPs, such as Pexiganan a magainin 2 analogue, have advanced to clinical trials [2]. The trials are, however, generally focused on the topical application of these peptide therapeutics, because their cytotoxicity prevents their direct injection into the bloodstream.

The main obstacle to the development of AMPs as therapeutics with systemic applications is that many natural AMPs are not highly selective between microbial and host cells. For instance, well-studied peptides such as magainins, in spite of being active *in vitro*, showed weak antimicrobial activity in animal models of infection [2]. As sufficiently high doses needed to effectively kill the invading pathogens, they may kill the host cells. "Good" AMPs should be both active (killing the microbes effectively) and selective (being able to discriminate host cells).

Along this line, there have been many attempts to optimize the activity and selectivity of AMPs by tuning their physiochemical properties such as peptide charge and hydrophobicity [5, 6, 7]. A comprehensive review can be found in Ref. [8]. Taheri-Araghi and Ha, using a coarse-grained model of peptide-lipid systems, showed that antimicrobial activity and selectivity of AMPs is optimized at a peptide charge $\hat{Q} \gtrsim 4$ in a salt-concentration dependent manner: the higher the salt concentration, the larger the $\hat{Q}$ [9]. As pointed out recently [8], however, it is not clear how cell concentrations are implicated in the selectivity.

Despite its significance, the cell selectivity has not been critically examined. In particular, how cell concentrations are implicated in the selectivity remains to be clarified. In this thesis, we propose a physical model for cell selectivity of AMPs, which enables us to examine its dependence on cell concentrations. Obviously, partitioning of peptides among target cells depends on the cell concentration, since different cells compete to recruit peptides. As detailed in this thesis, this suggests that the activity and selectivity of AMPs diminishes as the cell concentration increases. An important lesson of our studies presented here is that cell selectivity analysis needs to be done with caution – with appropriate choices of host and microbial cell concentrations.

1.2 Antimicrobial peptides

AMPs are ubiquitously found in nature. All living organisms including animals, plants, humans and bacteria use AMPs as part of their innate immunity to protect themselves against the invading pathogenic microbes [10]. These gene encoded molecules are similar to proteins in structure, however they are shorter in size (< 100 amino acids) and are thus, so to speak, short proteins. The structural diversity among AMPs is so huge that it is not easy to classify them based on their amino acid sequence. So far, more than 800 AMPs have been discovered, each with a different sequence [2]. Nevertheless, AMPs are classified into four main classes based on the conformation they adopt upon binding to lipid membranes: α-helical, β-sheet, loop, and extended peptides [11]. The first two classes are the most abundant in nature. Examples include helical magainin and β- sheets of tachyplesins isolated from the skin of the African clawed frog *Xenopus laevis* and horseshoe crab hemolymph, respectively [12].

The physiochemical properties of proteins and peptides are related to the sequence of the amino acids in their structure [13]. There are 20 standard amino acids in nature with different characteristics, as listed in Table 1.1 (adapted from Ref [14]). Despite a large sequence diversity, AMPs share some common characteristics such as a net positive charge and amphiphilicity [8] . Their positive charge is due to the presence of several basic residues in their structure such as lysine and arginine [10]. The cationic charge of AMPs is known to be responsible for their cell selectivity toward microbes, because the membranes of bacteria are more negatively charged than that of host cells.

AMPs have a distinct amphiphilic structure [10], that is, their sequence contains both hydrophilic (polar) and hydrophobic (nonpolar) residues, located on opposite sides of the molecule. The amphiphilicity of peptides enables them to interact effectively with lipid membranes as they also have an amphiphilic structure. Indeed, hydrophobic interaction between the hydrophobic face of the peptides and the hydrophobic core of the lipid membrane is the dominant interaction between peptides and host cells [8]. In other words, hydrophobicity of AMPs is one of the key parameters to control their cytotoxicity. Melittin, discovered in bee venome, is more toxic to mamalian cells compared to magainin,

Table 1.1: Amino acids and their physiochemical properties

Amino acid	3-letter name	side-chain polarity	net charge
Alanine	Ala	nonpolar	0
Arginine	Arg	polar	+1
Asparagine	Asn	polar	0
Aspartic acid	Asp	polar	-1
Cysteine	Cys	nonpolar	0
Glutamic acid	Glu	polar	-1
Glutamine	Gln	polar	0
Glycine	Gly	nonpolar	0
Histidine	His	polar	0
Isoleucine	Ile	nonpolar	0
Leucine	Leu	nonpolar	0
Lysine	Lys	polar	+1
Methionine	Met	nonpolar	0
Phenylalanine	Phe	nonpolar	0
Proline	Pro	nonpolar	0
Serine	Ser	polar	0
Threonine	Thr	polar	0
Tryptophan	Trp	nonpolar	0
Tyrosine	Tyr	polar	0
Valine	Val	nonpolar	0

which is believed to be due to its higher hydrophobicity. Several studies have also revealed that reducing peptides hydrophobicity reduces their hemolytic activity [8, 15, 16].

1.2.1 Mechanism of action

In general, AMPs are known as bacteriocidal agents that kill the microbes as oppose to bacteristatics, which just stop the growth of bacteria [10, 17]. Their cell-killing activity is fast; some peptides such as magainin 2 and cecropin PI have been shown to kill the bacteria in 15-90 minutes [17].

Despite extensive studies on AMPs, their exact microbial killing mechanism is not yet clearly understood. However, it is known that they are pore formers that target the cyto-

plasmic membrane of bacteria [10, 18]. Examples include magainin2, melittin, cecropin and alamethicin. As discussed in reference [17], there are three main steps involved in bacterial killing mechanism of AMPs: (i) attraction, (ii) attachment, (iii) membrane permeability.

Attraction

Peptides should be attracted to bacteria in order to kill them. In fact, this step is related to one of the most significant features of antimicrobial activity of AMPs, known as cell selectivity, the ability to recognize the bacteria in a crowd of host cells [10]. The underlying mechanism is electrostatic attraction between the peptides and the cell membranes [17]. Peptides are typically positively charged. In contrast, the outer leaflet of the outer membrane of bacteria is abundant in anionic lipids while host cells are almost neutral on their outer layers [10]. Thus strong electrostatic attractions between the cationic peptides and negatively charged bacterial membranes enables them to recognize bacteria as their main target [19].

Attachment

Electrostatic interactions bring AMPs into close proximity of lipid bilayers. The distinct amphiphilic structure of peptides then facilitates their hydrophobic binding to the cell membrane [17]. They attach to the membrane to establish the hydrophobic interaction between their hydrophobic side and the hydrophobic tails of lipids. According to the thorough experiments of Huang *et al.* on interaction of AMPs with model membranes, there are two binding modes for peptides on the membrane [20]. Their oriented circular dichroism (OCD) studies showed that, at low peptide to lipid ratios P/L, peptides lie parallel to the plane of the membrane [21]. They are indeed embedded in the interface between the lipid headgroups and tails, and stretch the membrane as was observed in the membrane thickness measurements [22]. They observed that membrane thickness reduces as the concentration of the peptides increases [23]. Since the volume of the hydrophobic core of

the membrane (lipid chains) is conserved, membrane thinning happens as a consequence of its area stretch. Nevertheless, membrane thickness remains constant above some threshold concentration of peptides P/L^*, which implies a different type of peptide-lipid interaction. Furthermore, orientation of bound peptides changes above this threshold concentration, and they are inserted perpendicular to the membrane (second binding mode)[22]. This peptide reorientation is concomitant with the formation of transmembrane pores [22].

Membrane permeability

As the concentration of bound peptides increases, the peptide-induced stress in the membrane also increases. Above the threshold P/L^* the membrane is disrupted to relieve the built-up tension. Although the exact membrane permeability activity of peptides is not yet clear, some models have been proposed to explain how they disturb the membrane. In what follows, we briefly discuss the models.

As summarized in reference [17], AMPs either form pores in the membrane or deteriorate the integrity of the membrane by micellization in a detergent-like way. Both mechanisms eventually lead to cell death. Pore former peptides rupture the cell membrane via two different types of pore: *toroidal* pores and *barrel-stave* pores [24]. Figure 1.1 shows the different types membrane-disruption mediated by AMPs.

In *toroidal* pores, peptides are inserted perpendicularly into the membrane and induce the lipid monolayers to bend continuously in such a way that the pore lumen is partly lined by peptides and partly by lipid head groups [25]. In this type of pores, as seen in Fig. 1.1 the charged (hydrophilic) side of the peptide faces the bilayer and lipid headgroups. Toroidal pores are highly curved structures that are stabilized due to the presence of peptides in the pore [26]. Magainin is one of the AMPs that forms toroidal pores in the lipid bilayer. Magainin pores are large and each pore includes 4-7 magainins [17].

In contrast, there exists the *barrel-stave* pores, which are uniquely formed by the antimicrobial peptide alamethicin [17, 25]. These peptides align perpendicular to the membrane and associate to form a bundle (much like a barrel of peptides), which is oriented parallel

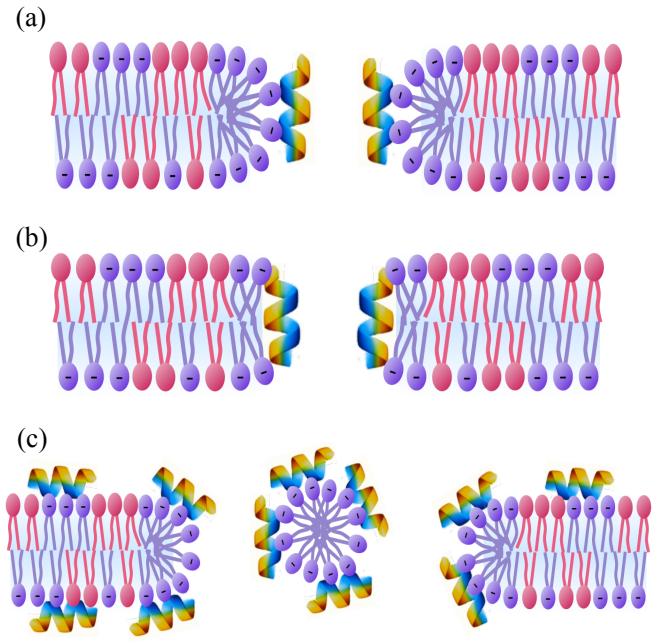

Figure 1.1: Illustration of different types of pores induced by α-helical peptides (adapted from Ref. [1]) The hydrophilic side of the helical peptide is shown in blue and the hydrophobic side in orange. (a) In toroidal pores, the hydrophilic side of the peptide faces the lipid bilayer and the hydrophobic side faces water. (b) In barrel-stave pores, the hydrophobic side of the peptide faces the lipid bilayer and the hydrophilic side is exposed to water. (c) In the carpet model, the membrane is covered extensively by the peptides and eventually micelles are created.

to the phospholipid tails. This transmembrane pore is lined by peptides only and, unlike the toroidal pores, the hydrophilic regions of the peptides form the edges of the pore. Barrel-stave pores are smaller than toroidal pores. The number of peptides in the pores is estimated to be 3-11, depending on the bilayer lipid composition [17].

There is another AMP-induced membrane disruption mechanism called *carpet model* [18]. In this model, peptides tend to reside parallel to the plane of the membrane. They largely cover the surface of the membrane in a carpet-like manner. At high concentration of peptides, they disintegrate the membrane and eventually form micelles similar to the effect of detergents. Ovispirin is an AMP that uses this mechanism of action [17].

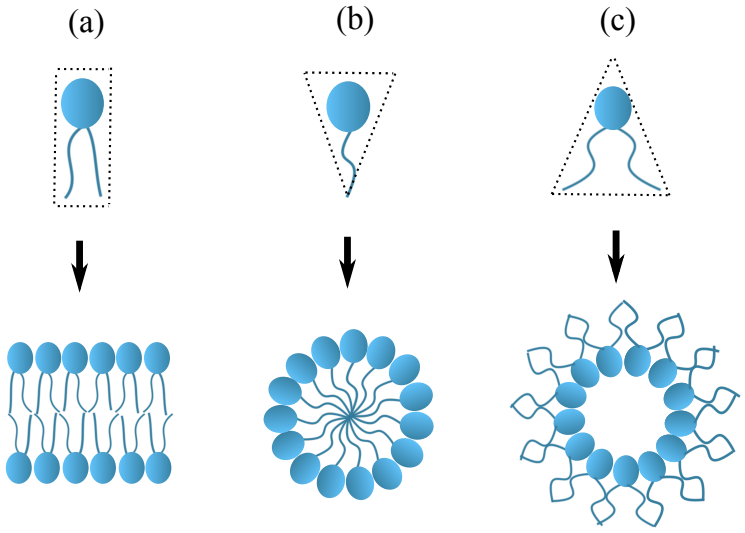

Figure 1.2: Illustration of the different self-assembly structures of lipids. Once there is *enough* lipids in solution, they self assemble in a shape-dependent manner: (a) The so-called cylindrical lipids, such as PC, form bilayer, (b) inverted-cone shaped lipids like lysolipids tend to form micelles, (c) cone-shaped lipids like PE form inverted micelles.

1.3 Cell membrane and lipid bilayer

Cells are the fundamental units of life. They are microscopically categorized into two groups: *prokaryotic* and *eukaryotic* [13]. Bacteria are the best representatives of the first group. The second group, eukaryotes, includes all the cells in animals, plants and fungi. Prokaryotic cells are generally smaller than eukaryotes. In both types of cell there is a membrane (cytoplasmic membrane) that encapsulates the cytoplasm and other intracellular components [27]. The membrane is mainly made of a lipid bilayer [13].

Lipids are amphiphilic molecules that consist of hydrophilic (polar) and hydrophobic (nonpolar) components, usually referred to as lipid head group and lipid tails, respectively. In aqueous solutions, they self-assemble into structures where the hydrophilic parts shield the hydrophobic parts from water molecules. The preferred structure is determined by size, shape, and the concentration of lipids [27]. As depicted in Fig. 1.2, it can be a lipid bilayer, a micelle, or an inverted micelle. The most abundant lipids in all cell membranes

are *phospholipids*. They have two fatty acid tails and also all of them have a phosphate group in their headgroups. A schematic view of phospholipid molecules can be seen in Fig. 1.2.

It is worth noting that the lipid curvature, which will be discussed in the third chapter, is in fact related to the curvature of its preferred self-assembly. Lipids that tend to form lipid bilayers are known to have a zero curvature. Positively and negatively curved lipids prefer the micelle and the inverted micelle structures, respectively.

1.4 Bacteria

Bacteria along with eukaryotes and archae constitute the three major forms of life. They are prokaryotic cells. Due to their small size, which is on the order of micrometers (μm), they are often referred to as microorganisms. Based on their shapes, bacteria are divided into three major groups: rods, spheres, and spirals.

As discussed previously, both bacteria and eukaryotes have a so-called cytoplasmic membrane (lipid bilayer) that surrounds the cell. In eukaryotes, it is only this lipid bilayer that separates the inside of the cell from the outside. However, in case of bacteria, there is a cell wall on top the lipid membrane as well, which mainly acts as protection for the cell. There are two major types of cell walls; based on the cell walls, bacteria are classified into two groups: *Gram-positive* and *Gram-negative* [13]. A schematic view of different cell walls is shown in Fig. 1.3. The so-called gram-staining property of bacteria is, in practice, determined by their response to some test dyes.

For Gram-positive bacteria, the cell wall contains a thick layer of *peptidoglycan*, a copolymer made of amino acids and sugars. Due to this peptidoglycan layer, they can retain the violet dye used in gram-staining tests, and are thus called gram-positive.

The cell walls of gram-negative bacteria are made of an outer membrane as well as a peptidoglycan layer. In other words, these bacteria have two membranes: the inner membrane (cytoplasmic membrane) and the outer membrane (see Fig. 1.3). There is a layer of peptidoglycan in between the two membranes which is thinner than that of the

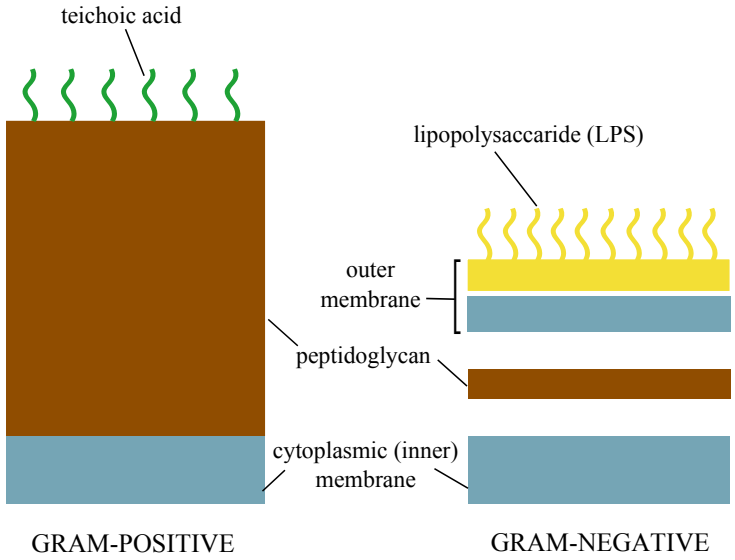

Figure 1.3: Schematic view of the membrane structure of Gram-positive and Gram-negative bacteria. In both cases, there is a cytoplasmic membrane (inner membrane), which is composed of phospholipids. However, Gram-negative bacteria have an outer membrane as well, which its inner leaflet is made of phospholipids, while the outer leaflet is made of a different type of lipids known as lipopolysaccharides.

gram-positive bacteria. Thus, they fail to retain the dye in the gram-staining procedure, and are called gram-negative. The inner membrane is the plasma lipid membrane, mostly made of phospholipids. The outer membrane has a somewhat different structure; the inner leaflet is made of phospholipids, and the outer leaflet is comprised of another type of lipid called *lipopolysaccharide* (LPS)[28].

Note that the main target of AMPs, in their microbe killing mechanisms, is the cytoplasmic membrane of bacteria. Thus, in the case of gram-positive bacteria, AMPs should pass across the peptidoglycan layer to reach the membrane. For gram-negative bacteria, however, they should pass across the outer membrane as well as the peptidoglycan layer before they can interact with the cytoplasmic membrane.

1.5 Overview of the thesis

The first chapter of this thesis is an introduction of the motivation and goals of this work. It is then followed by a brief overview of antimicrobial peptides (AMPs), their mechanism of action, structure of cell membranes, and bacteria.

In the second chapter, we describe the electrostatics for electrolyte solutions. The analytical tools to study the electrostatic interaction of such solutions, the Poisson-Botzmann equation and its linearized form the Debye-Huckel equation, are discussed in this chapter.

The third chapter is dedicated to the coarse-grained semi-analytical model we developed to consider the implication of cell concentration in activity and selectivity of AMPs. More specifically, using the Poisson-Boltzmann theory for charged surfaces, we study the interaction of peptides with a demixable lipid membrane. We will discuss how considering more than one lipid membrane, equivalent to considering a density of target cells, affects the selective membrane-disruptive activity of AMPs. We then developed a single-binding site approach to simulate peptide-membrane interactions. In this model, peptide binding is driven by a fixed binding energy and there is no interaction between the bound peptides on the membrane. In the end, we compare the results of this model with the results of the coarse-graining. Since the coarse-grained approach is mainly based on electrostatic interactions, the comparison indicates the effect of electrostatic interactions in the cell-concentration dependence of peptide activity and selectivity.

Chapter 2

Electrostatics for electrolyte solutions

2.1 Poisson-Boltzmann theory

Electrostatic interactions play important roles in determining the structure and function of biological systems in aqueous solution. For instance, the presence of multivalent counterions can induce condensation of negatively charged DNA molecules into ordered structures [29]. In addition, electrostatic interactions often control molecular association between charged objects. For instance, cationic antimicrobial peptides preferentially bind to membranes carrying anionic lipids such as bacterial cell membranes [12]. The potency of these peptides as therapeutic agents relies on this selectivity, as detailed in the next chapter.

In this chapter, we present Poisson-Boltzmann (PB) theory, a standard mean field approach to charged systems in an electrolyte solution. Here, our consideration is limited to the simple case of a uniformly-charged surface interacting with mobile ions. Such a consideration will be useful for developing an adequate theoretical approach to more complicated systems introduced in the next chapter.

Any substance that dissolves into ions in a polar solvent like water is called an electrolyte and the resulting ionic solution is called the electrolyte solution [30]. The electrostatic interactions among charged molecules in an electrolyte solution are not solely determined

by their direct Coulomb forces but are screened by the surrounding dissolved ions. An anionic molecule, for instance, tends to be surrounded by cationic ions (e.g., Na^+). The anionic charge is thus "shielded" by an ionic cloud of opposite charge, forming the so-called diffusive layer. As a result, the electric potential due to the anionic charge is screened and weakened.

The equilibrium distribution of ions in solution is determined by the balance between energy and entropy. In statistical mechanics, the distribution of the ions is obtained using the Poisson-Boltzmann (PB) equation captures this at the mean-field level. It is a differential equation that determines simultaneously the charge density and the electrostatic potential at the same point inside the solution. It is basically derived from the Poisson equation combined with the Boltzmann distribution function.

In electrostatics, the relation between the electric potential $\psi(\mathbf{r})$ and the charge distribution is given by the Poisson equation

$$\nabla^2\psi(\mathbf{r}) = -\frac{\rho(\mathbf{r})}{\epsilon_0\epsilon_w} = \frac{-e}{\epsilon_0\epsilon_w}\sum_i z_i n_i \tag{2.1}$$

where $\rho(\mathbf{r})$ is the total charge density at $\mathbf{r}$, ϵ_0 the electric permittivity of vacuum and ϵ_w the dielectric constant of the aqueous solution. The second equation describes the total charge density in an electrolyte solution containing different ion species denoted by i. Each ion has a number density of $n_i(\mathbf{r})$ and a charge of number $-ez_i$ with $-e$ the electrostatic charge and z_i the charge (valence) number.

In statistical thermodynamics, ions in electrolyte solution are assumed to obey Boltzmann statistics. Thus, the density of ions at position $\mathbf{r}$ is related to the probability of finding them at $\mathbf{r}$ which is given by Boltzmann factor.

$$n_i(\mathbf{r}) = n_i^0 \exp(-ez_i\psi(\mathbf{r})/k_BT) \tag{2.2}$$

Where n_i^0 is the density of ion i at infinity ($\lim_{\mathbf{r}\to\infty}\psi(\mathbf{r}) = 0$). The exponential argument indeed gives the electrostatic energy of the ith ion at $\mathbf{r}$, with k_B the Boltzmann constant and T the temperature.

By substituting ion distributions from Eq. 2.2 into the Poisson equation Eq. 2.1 we obtain the well known Poisson-Boltzmann equation.

$$\nabla^2\psi(\mathbf{r}) = \frac{-e}{\epsilon_0\epsilon_w}\sum_i z_i n_i^0 \exp(-ez_i\psi(\mathbf{r})/k_BT) \tag{2.3}$$

We can assume for simplicity that there is just one type of counterion with number density of n_0^+ and valence z_+ and one type of co-ion with n_0^- and z_-. For such ionic solution the PB equation is reduced to

$$\nabla^2\psi(\mathbf{r}) = \frac{-e}{\epsilon_0\epsilon_w}\big(z_+n_0^+ \exp(-ez_+\psi(\mathbf{r})/k_BT + z_-n_0^- \exp(-ez_-\psi(\mathbf{r})/k_BT\big) \tag{2.4}$$

In a 1:1 electrolyte solution such as NaCl, which is also the case in this thesis, we have $n_0^+ = n_0^- = n_0$ and $z_- = -z_+ = -1$. Eq, 2.4 is then further simplified as

$$\nabla^2\phi(\mathbf{r}) = \kappa^2 \sinh[\phi(\mathbf{r})] \tag{2.5}$$

Where $\phi = e\psi/k_BT$ is the reduced electrostatic potential and κ is the inverse of Debye screening length defined as $\kappa^2 = (\frac{1}{\lambda_D})^2 = 8\pi e^2 n_0/4\pi\epsilon_0\epsilon_w k_BT$. It is more common to write $\kappa^2 = 8\pi l_B n_0$ with l_B the Bjeruum length defined as, $l_B = e^2/4\pi\epsilon_0\epsilon_w k_BT$. In fact, the Bjeruum length is the separation between two elementary charges in an ionic solution with dielectric constant ϵ_w at which their electrostatic interaction is comparable to the thermal energy.

2.2 The linearised PB equation: Debye-Huckel theory

When the charged bodies inside the solution are weakly charged ($e\psi(\mathbf{r}) \ll k_BT$) we can use Taylor expansion to expand the PB equation Eq. 2.5 to the first order of ϕ *i.e.,* $\sinh(\phi) \approx \phi$. The resulting linearised form of the PB equation is known as the Debye-Huckel equation

$$\nabla^2\phi(\mathbf{r}) = \kappa^2\,\phi(\mathbf{r}) \tag{2.6}$$

Here, $\phi(\mathbf{r}) = e\psi/k_BT$ is the reduced potential, however, needless to say that the same equation holds for the electric potential $\psi(\mathbf{r})$ as well. This linear second order differential equation is analytically solvable for different geometries. Let us consider the simple scenario of an infinitely extended planar membrane with uniform surface charge density σ which is depicted in Fig. 2.1. Due to the symmetric configuration of the membrane in the (x, y) plane, the electric potential is just a function of z. Requiring zero potential at far distances from the membrane ($\lim_{\mathbf{r}\to\infty} \psi(\mathbf{r}) = 0$), and a constant electric field on the surface $\nabla\psi(0) = -\sigma/\epsilon_0\epsilon_w$, the solution of the Eq. 2.6 is

$$\psi(z) = \frac{\sigma}{\epsilon_0\epsilon_w\kappa} \exp(-\kappa z). \tag{2.7}$$

The effect of salt ions in the potential is seen through κ. Electrostatic potential is exponentially decreasing due to the screening effect of the salt ions in the ionic solution. As seen in Eq. 2.7, electrostatic interactions are effectively suppressed beyond the Debye screening length (when $\kappa z > 1$). The screening length is related to the salt concentration, $\kappa^{-1} = (8\pi l_B n_0)^{-1/2}$. It varies from around 3 $\mathring{A}$ for 1 M of a (1:1) electrolyte (*e.g.,* NaCl) to about 1 μm for pure water (with H^+ and OH^- ions).

2.3 The Poisson-Boltzmann equation in planar geometry

The Debye-Huckel theory is valid for low potential surfaces (smaller than 25 mV at room temperature), but for highly charged surfaces the original PB equation (see Eq. 2.5) is better suited than the DH theory. In general, the PB equation is a nonlinear equation which is numerically solvable for different boundary conditions. It can, however, be solved analytically for a planar geometry. As discussed in Ref. [31], the PB potential on the surface of a planar membrane with surface charge density σ is given as

$$\phi_0 = 2\,\sinh^{-1}\left(\frac{2\,\pi\sigma l_B}{\kappa}\right) \tag{2.8}$$

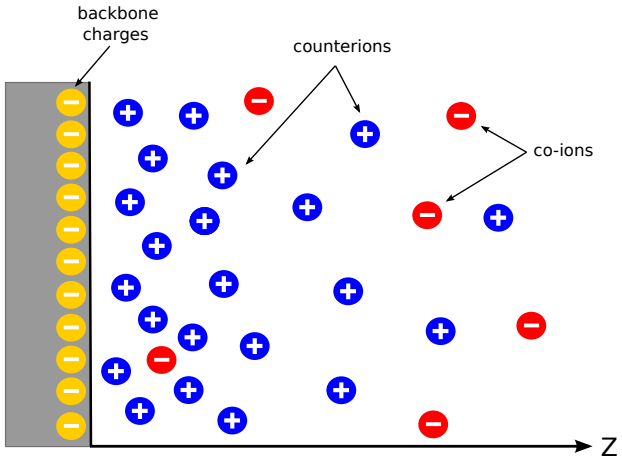

Figure 2.1: Charged membrane with negative surface charge density in a salty solution. The planar membrane is infinitely extended in the (x, y) plane where its orthogonal cross section normal to the y axis is illustrated here. Due to the presence of the charged membrane a density profile of $n_{\pm}(z)$ is created for cations and anions. In the vicinity of the membrane, the density of the counterions is increased while the density of the co-ions (like-charged ions) is decreased.

where $\phi_0 = e\psi_0/k_BT$ is the reduced surface potential.

The advantage of having the surface potential is that we can now calculate the electrostatic free energy of the membrane F, using the so-called Debye charging process: in this method, the free energy is given by the work that is done to charge up the membrane from 0 to its final surface charge density σ

$$F = A \int_0^{\sigma} \psi_0(\sigma')\, d\sigma' \tag{2.9}$$

where ψ_0 is the surface potential and A the area of the membrane. Using the surface potential given in Eq. 2.8, the charging free energy per unit area of the planar membrane is obtained as

$$F_e(\sigma) = \sigma\, \phi_0 - \frac{\kappa}{\pi\, l_B} \left[\cosh\left(\frac{\phi_0}{2}\right) - 1 \right] \tag{2.10}$$

where F_e describes the total electrostatic free energy of a membrane which carries a surface

charge density σ and is immersed in an ionic solution with screening length κ. Eq. 2.10 is one of the key equations throughout this thesis; in fact, it will be used to compute the free energy of the membrane in our modelling . It is worth noting that entropy of the salt ions and their contribution to the electrostatic energy is also incorporated in F_e. In other words, calculation of the free energy using Debye charging method (Eq. 2.9) is equivalent to the direct calculation of the membrane-solution system as

$$F = \frac{\epsilon_0 \epsilon_w}{2} \int [\nabla \psi(\mathbf{r})]^2 d\mathbf{r} + k_B T \int \Big[n_+ \ln \frac{n_+}{n_0} + n_- \ln \frac{n_-}{n_0} - (n_+ + n_- - 2n_0) \Big] d\mathbf{r} \quad (2.11)$$

Here, the first term gives the total electrostatic energy of the membrane-solution system with $\psi(\mathbf{r})$ the electric potential at $\mathbf{r}$. The second term describes the entropy of the salt ions. In this term, n_+ (n_-) is density of the cationic (anionic) ions and n_0 density of the salt ions far from the membrane at $z = +\infty$ ($\psi = 0$ *at* $z = +\infty$).

Equality of the two different methods to calculate the free energy given in Eq. (2.9) and Eq. (2.11) can be easily shown using the DH theory. To do so, we consider a planar membrane with low surface charge density similar to the one we already discussed in section 2.2, and calculate its free energy using DH theory in two alternative ways.

Let us first consider the Debye charging method. The DH potential for the planar membrane in a salt solution is given in Eq. 2.7. The surface potential then reads $\psi_0(z = 0) = \sigma/(\epsilon_0 \epsilon_w \kappa)$. Substituting the surface potential into the charging free energy in Eq. 2.9 we have

$$\frac{F_{DC}}{A} = \int_0^\sigma \frac{\sigma}{\epsilon_0 \epsilon_w \kappa} \, d\sigma = \frac{\sigma^2}{2\epsilon_0 \epsilon_w \kappa} \quad (2.12)$$

where F_{DC} is the electrostatic charging free energy per unit area of the membrane.

Let us now compute the free energy of the planar membrane using the alternative method given in Eq. 2.11; the two terms in the free energy (the electrostatic energy and the entropy of the salt ions) are calculated separately. Using the DH potential for the planar geometry in Eq. 2.7, the electrostatic energy of the system is given as

$$\frac{\epsilon_0 \epsilon_w}{2} \int [\nabla \psi(\mathbf{r})]^2 d\mathbf{r} = \frac{\epsilon_0 \epsilon_w}{2} A \int_0^\infty \big[- \frac{\sigma}{\epsilon_0 \epsilon_w} \exp(-\kappa z) \big]^2 dz = \frac{A\sigma^2}{4\epsilon_0 \epsilon_w \kappa} \quad (2.13)$$

To calculate the entropy of the salt ions, we need to know their spatial distribution (density as a function of position $\mathbf{r}$). As discussed in Sec. 2.1, the density of the cations and anions is related to their Boltzmann weight

$$n_{\pm}(z) = n_0 \exp(\mp e\psi(z)/k_B T) \tag{2.14}$$

where $\psi(z)$ is the electric potential; here we use the DH potential in Eq. 2.7. Using their number densities $n_{\pm}(z)$, the entropy of the salt ions is calculated as (the details of the calculation is found in appendix A)

$$\int \Big[n_+ \ln \frac{n_+}{n_0} + n_- \ln \frac{n_-}{n_0} - (n_+ + n_- - 2n_0) \Big] d\mathbf{r} = \frac{A\sigma^2}{4\epsilon_0 \epsilon_w \kappa} \tag{2.15}$$

The electrostatic free energy of the membrane-solution system is now obtained by summing up the electrostatic energy in Eq. 2.13 and the entropy of the salt ions in Eq. 2.15.

$$\frac{F}{A} = \frac{\sigma^2}{4\epsilon_0 \epsilon_w \kappa} + \frac{\sigma^2}{4\epsilon_0 \epsilon_w \kappa} = \frac{\sigma^2}{2\epsilon_0 \epsilon_w \kappa} \tag{2.16}$$

which is equal to the free energy we computed using Debye charging method in Eq. (2.12). This equality assures us that the contribution of the salt ions in free energy is included in the charging free energy. In principle, we can expand this conclusion to the original nonlinear PB theory and the charging free energy in Eq. (3.6).

It is worth noting that PB and DH theories rely on some important assumptions: i) the solvent is considered as a continuous medium with a constant electric permittivity (dielectric constant), ii) the finite size of the ions is ignored and they are assumed as point charges, iii) the only interactions between charged bodies is taken to be Coulomb interactions, iv) any dipole-dipole interaction is neglected, v) the density profile of all ions $n_i(\mathbf{r})$ is a continuous function of $\mathbf{r}$. Another significant note is that PB and DH approaches neglect the local fluctuations of the charge densities and are thus called mean field theories. These mean field approaches are, in general, good approximations at most physiological conditions specially for monovalent ions. In the case of multivalent ions, however, the

mean field PB should be modified to account for charge-charge correlations because they are important for multivalent ions.

In this thesis, we deal with a symmetric (1:1) electrolyte solution, but on the membrane we consider lipid demixing which is a consequence of charge-charge correlation. In order to incorporate the lipid demixing, we have adopted a non-trivial way within the PB framework which will be discussed in greater detail in the next chapter.

Chapter 3

Effect of cell concentration in activity and selectivity of antimicrobial peptides

3.1 Introduction

Many cationic peptides such as magainin 2 [26] and melittin [32] (two of the best studied AMPs) kill bacteria in an all-or-none concentration-dependent manner by forming pores on the bacterial membrane. But some peptides employ intracellular killing mechanisms against microbes [17]. For instance, dermaseptin inhibits nucleic-acid synthesis [17]. Nevertheless, membrane lytic peptides are of significant interest, because they use a non-specific mechanism [12, 10] and thus do not easily induce bacterial resistance. Acquiring resistance would require the "expensive" work of redesigning lipid membranes [10].

One significant feature of AMPs is their cell selectivity, which enables them to preferentially bind to and kill microbes over the host cells [4, 12]. AMP's cell selectivity is often measured by the so-called therapeutic index: the ratio between their minimum hemolytic concentration (MHC) and their minimum concentration at which bacterial growth is inhibited (MIC) [5]. The higher the therapeutic index, the more effective the AMP would

be as an antibiotic. In general, peptide selectivity (therapeutic index) is improved by decreasing their hemolytic activity (higher MHC) or enhancing their bacterial activity (lower MIC). Accordingly, there have been many attempts to find the parameters that control the selectivity of AMPs (a comprehensive review can be found in [8]).

Despite its significance in determining the cell selectivity, however, the cell-concentration dependence of AMP activity has not yet been criticality examined. As pointed out in reference [8], some confusion remains to be resolved, since the selectivity has often been measured with different densities of host cells and bacteria. Host cell densities used in some hemolytic assays are sometimes three orders of magnitude larger than those of bacteria [8]. As a result, the selectivity is overestimated. Therefore, a systematic understanding of how cell densities would affect the activity and selectivity of AMPs is highly desirable. Here we offer guiding principles that underlie the cell-concentration dependence of AMP's membrane-perturbing activity and selectivity. To this end, we present a coarse-grained model that captures such molecular details as lipid composition and peptide amphiphilicity-charge.

In this work, the lipid composition of a membrane refers to a varying fraction of anionic lipids. Cationic peptides interact with such a membrane electrostatically or hydrophobically. They can form a diffusive layer like multivalent cations or can insert into the interface between headgroupds and lipid tails in a parallel orientation (with respect to the interface); at high concentrations, they will eventually orient themselves perpendicularly to form pores [22].

Despite uncertainties about AMP's microbe-killing mechanisms, their interaction with membranes deserves much consideration, since the membrane is the first barrier to cross. Here the main focus is on clarifying how the electrostatic "discrimination" of cationic AMPs between microbial and host cell membranes varies with cell densities, using the aforementioned simplified model of peptide-membrane systems. Our effort will help understand experiments, especially with model membranes, and resolve conflicting views on cell or membrane selectivity of AMPs [8].

In this chapter, we first develop a free energy approach to the model system and examine

the effect of cell densities on the cell selectivity of AMPs. Results for MHC and MIC are discussed in detail and the cell-density dependence of the selectivity is analysed.

3.2 Molecular model

Although the exact mechanism of action of AMPs has not been fully understood yet, the main physiochemical properties of peptides required for bacterial discrimination and membrane-disruption have been identified as follows.

i) **Cationic charge**, The majority of AMPs possess high levels of cationic residues in their primary amino acid sequence which enables them to strongly interact with anionic membrane of bacteria [33]. This cationic charge is also the key tool for cationic AMPs to specify the anionic membrane of bacteria in a crowd of host cells with almost neutral membranes [10].

ii) **Amphiphilicity**, Another common feature of AMPs is their amphiphilic structure that is their amino acid sequence constitutes both polar (hydrophilic) and non polar (hydrophobic) residues [33]. This structural feature gives antimicrobial peptides the ability to interact more efficiently with the phospholipid membranes having also an amphiphilic structure (hydrophilic lipid head group and hydrophobic tail).

We have captured these essential properties of AMPs in our coarse-graining. Our peptides are characterized by a cationic charge Q, and their hydrophobicity is appreciated by a hydrophobic energy (denoted as ϵ_I) contributing in the free energy of the system that is discussed later in this chapter.

Peptides are modelled as positively charged disks on the membrane and as random coils in bulk. In real lipid-peptide systems, peptides are unstructured in the electrolyte solution and they are folded to a secondary structure (very often an α-helix) upon binding to the membrane [34]. The reason is that binding of peptides to membranes is associated with an environmental change from the aqueous medium (water) to the hydrophobic phase of lipids.

Formation of an α-helix is generally easier in a hydrophobic environment than in water, because water destabilizes the intra-molecular hydrogen bonds. Thus, peptide binding is accompanied by a conformational transition, from random coil in water to an α-helix on the membrane [35, 34]. In our coarse-graining, the tendency for helical structure formation on the membrane is incorporated into the free energy gain for hydrophobic interaction with lipid tails, ϵ_I, since both of them are promoted in a lipidic environment.

In our approach, the lipid membrane is considered as a two-dimensional binary fluid mixture of anionic (*e.g,.* PG) and zwitterionic (neutral) lipids such as PC. Acidic lipids carry one electrostatic charge, -e, and for simplicity all the lipids are assumed to have the same head group area, a_l. Moreover, membrane proteins are not included in our coarse-graining. The surface charge density of the membrane is determined by the average fraction of anionic lipids denoted by $\bar{\alpha}$, that is more specifically, number of charged lipids/total number of lipids ($0 < \bar{\alpha} < 1$). In the absence of bound peptides, neutral and charged lipids are homogeneously mixed on the membrane. In this state, membrane is treated as a surface with uniform charge density of $\sigma = -e\,\bar{\alpha}/a_l$ with e the elementary charge and a_l the lipid headgroup area. However, biomembranes are actually fluid mixtures of lipids where lipids can move laterally in the plane of the membrane if needed. In the case of peptide binding on the membrane, lipid mobility allows anionic lipids to migrate to the vicinity of the cationic peptides. Thus, concentration of the charged lipids becomes higher in close proximity of the bound peptide so as to optimize the electrostatic interaction strength between the peptide and the membrane. This redistribution of lipids is known as *lipid demixing* [36]. In our approach we have treated this lipid demixing in a non-trivial way which will be elaborated later in this chapter.

The membrane is immersed in an ionic solution containing monovalent anions and cations (*e.g.,* $\mathrm{Na}^+$and Cl^-), with dielectric constant ϵ_w. It is basically the dielectric constant of water as the main component of this salty fluid. The electrolyte solution is in contact with a salt reservoir such that the salt concentration in bulk is fixed at n_0. Furthermore, the solution contains both peptides and membranes at finite concentrations.

Our approach considers two modes of binding for peptides on the membrane: Surface adsorption and hydrophobic insertion indicated by mode S and mode I, respectively. Pep-

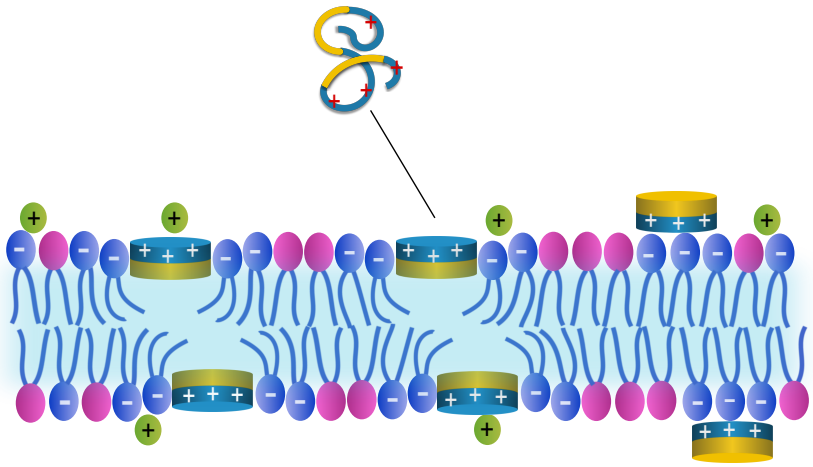

Figure 3.1: Illustration of peptides in different binding modes on the lipid bilayer. Peptides in binding mode I are inserted into the interface between lipid head group and tails. Peptides in binding mode S are electrically bound to the surface. In symmetric binding, peptides are evenly distributed between the inner and outer monolayers.

tides in binding mode S, are just electrically bound to the membrane where they form a diffuse layer. As shown in Fig. 3.1 they lie parallel to the plane of the membrane facing their hydrophilic charged side to the polar head group of lipids. Peptides in the state I are inserted into the lipid head group-tail interface exposing their hydrophobic part to the hydrophobic core of the membrane.

The main focus of this thesis is on the peptides in binding mode I, because they have a major role in the membrane disruption. They are inserted in the interface between lipid head groups and hydrophobic tails and consequently induce mechanical deformation in the membrane that, under the right conditions, leads to membrane rupture. Nevertheless, we consider the electrically bound peptides (in binding mode S) as well, since they affect the concentration of the peptides in binding mode I through energetics. Peptides in mode S compete with those in mode I to attract anionic lipids to their vicinities. This competition due to limited number of lipids on the membrane, as well as peptide-peptide repulsion between the peptides in different binding modes, influences the density of membrane-perturbing peptides (in mode I). Hence, the existence of peptides in binding mode S can

not be neglected.

3.3 Free energy calculation and Wigner-Seitz Cell approximation

In order to calculate the free energy of our peptide-membrane system, we have used a mean-field scheme where every bound peptide defines a circular cell, on the membrane, and the total free energy is the summation of the free energy of individual cells. The total number of the cells is equal to the number of the bound peptides on the membrane.

As evidenced in experimental works, the density of bound peptides is typically high enough that peptide-peptide interactions cannot be neglected [37, 38]. In fact, once there are a large number of peptides on the membrane, there is accordingly a stiff 'competition' between bound peptides to attract anionic lipids to their vicinities. Since the membrane is not an unlimited source of anionic lipids, the aforementioned competition results in an effective repulsion between like-charged peptides on the membrane. In order to minimize the electrostatic repulsion, peptides are believed to form a hexagonal lattice on the membrane [9]. Following the same idea, we have adopted a hexagonal lattice model for peptides bound onto the lipid bilayer. Based on this assumption, peptides on the membrane, regardless of the binding mode they are in, define a two-dimensional Wigner-Seitz cell (WSC) with radius R as depicted in Fig. 3.2. However, considering a circular WSC for peptides on the membrane is justified by the fact that biological membranes are actually fluid, and bound peptides can move on the plane of the membrane (especially when lipid tails are at the liquid phase) [9]. Therefore, any bound peptide on the lattice, on average, experiences a radially symmetric distribution of other bound peptides on the membrane which is captured in a round WSC for each peptide.

The Wigner-Seitz cell model has been widely used to describe the distribution of charged particles on charged surfaces. May, *et al.* have used such a cell model to describe the protein-protein and protein-lipid interactions of charged proteins (modelled as charges spheres) on the mixed lipid membranes [39]. Taheri-Araghi and Ha have also used this

method to consider the interactions of disk-shaped peptides (model of cationic AMPs) with each other and with the lipid membrane [9]. Considering the WS cell scheme for the distribution of charged peptides on the membrane is an approximation which is valid in two limiting cases: when the surface density of bound peptides is so low or when there are a large number of them on the membrane. In the former, peptide-peptide interactions are negligible and the system is reduced to a single peptide on the membrane. For such systems, there is no constraint on the arrangement of the bound peptides and any geometrical distribution works fine for the peptides on the membrane. At very high surface density of peptides, lateral interactions between peptides on the membrane are pronounced and they tend to arrange themselves into a hexagonal lattice on the membrane. In the intermediate level, however, accuracy of the cell model is reduced due to the lateral fluctuations of the bound peptides.

Here, we have adopted a semi-analytical approach to compute the free energy. More specifically, we use an analytical method to calculate the free energy of the WSC as a function of its radius R and peptide-membrane parameters.

In our cell model, each WS cell contains a uniformly charged disk (model of a peptide) with radius R_p at its center (see Fig. 3.2). The thickness of the peptides is suppressed, and in fact our approach can be extended to other geometries provided the thickness is neglected. The disk peptide is either adsorbed on the surface or inserted into the lipid headgroup-tail interface. All the cells, regardless of the binding mode of the peptide at their center, have the same area, A_{ws}, defined as

$$A_{ws} = \frac{1 + \sigma_I \, \mathcal{A}_P}{\sigma_I + \sigma_S} \tag{3.1}$$

where, $\mathcal{A}_P$ is the area expansion per inserted peptide, and $\sigma_I(\sigma_S)$ the area density of the peptides in binding mode I (S). Insertion of the membrane perturbing peptides (in binding mode I) at the interface between lipid headgroups and tails stretches the membrane analogous to the effect of an external tensile force, which will be elaborated later in this chapter. The membrane area increase is related to the density of peptides in binding mode I, $\Delta A/A = \sigma_I \, \mathcal{A}_P$, with A the area of the membrane. In other words, if all the

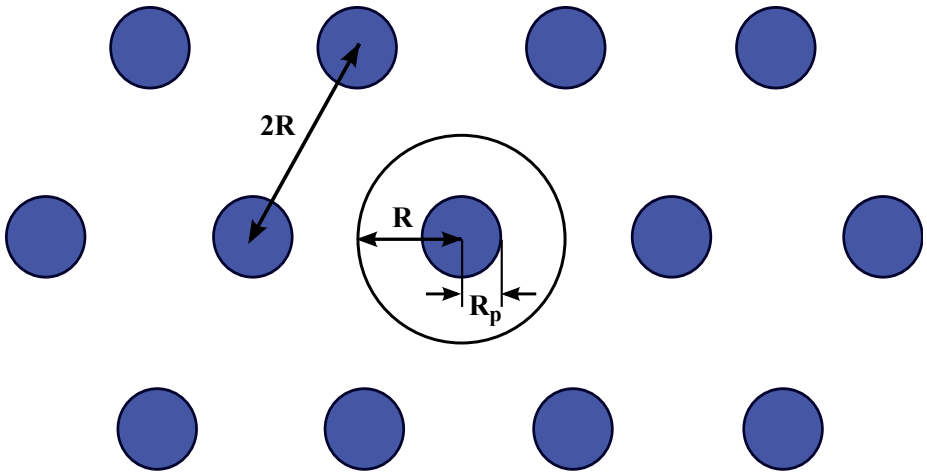

Figure 3.2: Illustration of peptides hexagonal lattice on the surface (top view)

bound peptides are in binding mode S ($\sigma_I = 0$), the area of the membrane will not change compared to that of the bare membrane (no bound peptide). However, the induced area expansion is evenly distributed within the whole plane of the membrane and thus the area of the WSC, for all bound peptides, is defined as the the total stretched area of the membrane divided by the total number of bound peptide as it is seen in the Eq. (3.1). Note that A_{ws} is not only a function of the total number of bound peptides but also the fraction of peptides in binding mode I. The more peptides in binding mode I, the higher the degree of membrane expansion and consequently the larger the area of each WS cell would be.

The only difference between cells with peptides at different binding modes is in their total number of lipids. There are more lipids in a cell consisting of a surface adsorbed peptide than that of an interface inserted one (in mode I). The reason is that penetration of the peptide in binding mode I to the lipid headgroup-tail interface will push away the surrounding lipids as schematically shown in Fig. 3.3

It is worth noting that in the cell model, peptide-peptide electrostatic repulsion on the membrane have been taken into account in the radius of the WSC, $R^2 = A_{ws}/\pi$, explained as follows. Energetically unfavourable repulsion interactions have a negative effect on

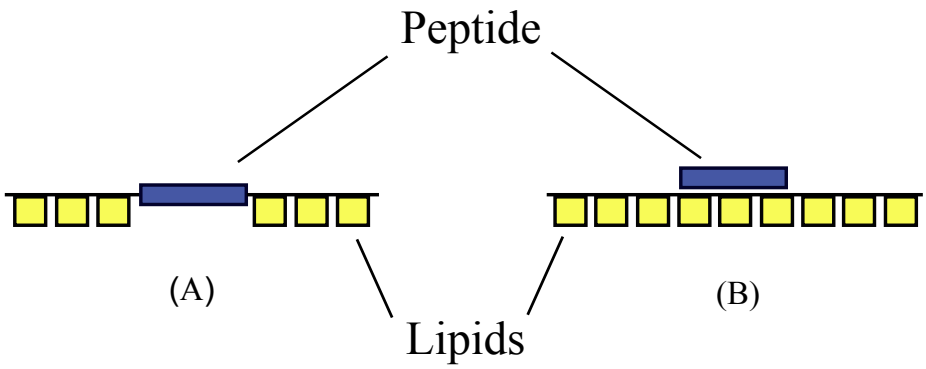

Figure 3.3: Illustration of peptide binding modes on the membrane (side view): (A) membrane inserted (binding mode I), (B) surface adsorbed (binding mode S).

peptide binding. In other words, the higher the inter-peptide electrostatic repulsion, the lower the number of bound peptides would be on the membrane which, according to the Eq. (3.1), corresponds to a larger radius for the WS cells. Therefore, smaller radii for the cells imply weaker repulsive interactions between bound peptides.

Our cell model also considers lipid rearrangement upon peptide binding, which is discussed in detail in the next section.

3.3.1 Lipid demixing

Membranes are fluid mixtures of anionic lipids which can move in the plane of the membrane and respond to peptide binding. When a cationic peptide binds to the membrane, anionic lipids are affected by its electric field and, because of their mobility, move towards the bound peptide to neutralize its charge and minimize the energy of the system. As discussed previously, this electrostatically-driven lipid rearrangement in the vicinity of bound peptides is called lipid demixing. Deviation of lipids from their homogeneous distribution, in lipid demixing process, is accompanied by an entropy penalty. The extent of lipid rearrangement around the bound peptide is indeed determined by the balance of the electrostatic energy gain and the entropy penalty of lipid demixing. In membranes with

very low surface charge density (e.g., $\bar{\alpha} = 0.05$) the demixing entropy penalty of lipids dominates the electrostatic energy gain especially for peptides with low charge density and thus lipid demixing is not very pronounced. In contrast, for membranes with higher charge density where for instance 20 percent of lipids are charged, lipid demixing has a significant role in peptide binding [39].

In our approach, as illustrated in Fig. 3.4, we assume that each WS cell is divided into two main regions: (i) Zone 1 consisting of the bound peptide and surrounding lipids with total area of A_s and α_1 fraction of anionic lipids. (ii) The second region, zone 2, which constitutes lipids only with α_2 ratio of anionic to neutral lipids.

If lipids are ideally mixed and the local charge modulation of lipids around the bound peptides is neglected, α_1 and α_2 will be the same and equal to the average fraction of charged lipids $\bar{\alpha}$. However, in the presence of lipid demixing, electrostatic migration of anionic lipids towards the bound peptide yields a higher fraction of charged lipids in the vicinity of the peptide, *i.e.*, $\alpha_1 > \alpha_2$. Nevertheless, these two quantities are not totally independent of each other and are found by minimization of the free energy subject to the constraint that the total number of charged lipids in each WS cell is conserved:

$$\int_{A_{ws}} (\alpha_i - \bar{\alpha})\, da = 0 \tag{3.2}$$

This integral is carried over the surface of the WSC. However, the lower limit depends on the binding mode of the peptide at the centre of the cell, which is 0 or A_p for adsorbed and inserted peptides, respectively. In the above integral, $\bar{\alpha}$ is the average fraction of charged lipids and α_i indicates the fraction of anionic lipids in each zone, *i.e.*, (i = 1, 2). Note that α_i of each region depends on the binding mode of the peptide as well, such that considering the α_1 as the independent variable, α_2 is outputted from the above constraint, as follows

$$\begin{aligned} \alpha_{2I} &= \frac{\bar{\alpha}\,(A_{ws} - A_p) - \alpha_{1I}\,(A_s - A_p)}{A_{ws} - A_s} \\ \alpha_{2S} &= \frac{\bar{\alpha}\,A_{ws} - \alpha_{1S}\,A_s}{A_{ws} - A_s} \end{aligned} \tag{3.3}$$

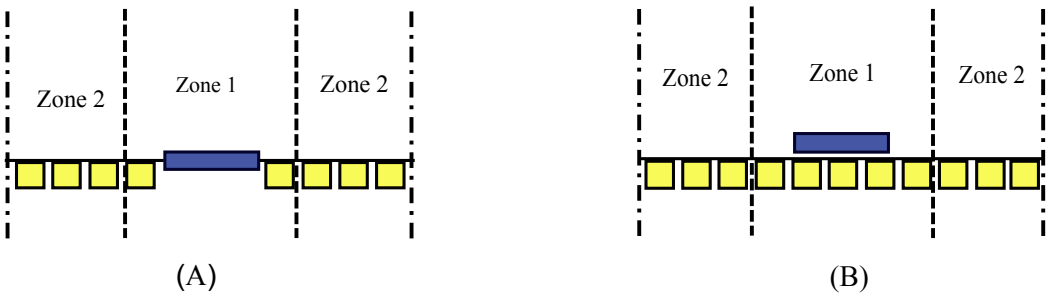

Figure 3.4: Schematic view of zone 1 and zone 2 of the WSC in the semi-analytical calculations. (A) The peptide at the center of the WS cell is interfacially bound to the membrane (binding mode I). (B) The bound peptide is adsorbed onto the surface (binding mode S). There are less number of lipids in Zone 1 for a peptide in the binding mode I compare to that of in the binding mode S.

Here, α_{2I} (α_{2S}) is the ratio of charged lipids in zone 2 of a WSC with a peptide at its center in binding state I (S). A_s is the area of the zone 1 and A_p is the area occupied by a bound peptide.

The area of the zone 1, A_s, is in principle determined by the peptide area and the area occupied by the surrounding lipids that effectively interact with the peptide. The area of this effective interaction region around the bound peptide, is read from the two-dimensional Debye screening length which was introduced by Velazquez and Blum [40]: $\kappa_2^{-1} = a_l/2\pi l_B \bar{\alpha}$, with a_l the lipid head group area, l_B the Bjerrum length and $\bar{\alpha}$ the average fraction of anionic lipids. Based on their theory, only lipids within this screening length interact with the bound peptide effectively. Therefore, for a disk-like peptide of area $A_p = \pi R_p^2$, zone 1 has the area of $A_s = \pi(R_p + \kappa_2^{-1})^2$.

All WS cells, irrespective of the binding mode of the peptide, have the same area for the zone 1, A_s, but different number of neutralizing lipids in this zone. Insertion of a peptide into the membrane would naturally push away the lipids and thus there are less lipids in the zone 1 of a WSC with a peptide in binding mode I compared to that of a peptide in binding mode S. Consequently, charge neutralization is stronger for the latter as seen in the Fig. 3.4.

For a bound peptide with cationic charge Q, the charge density of the zone 1 depends

on the peptide binding mode as following

$$\begin{aligned} \sigma_{1S} &= \frac{Q}{A_s} - \frac{\alpha_{1S}}{a_l} \\ \sigma_{1I} &= \frac{Q}{A_s} - \frac{\alpha_{1I}\,(A_s - A_p)}{a_l\,A_s} \end{aligned} \tag{3.4}$$

where, $\sigma_{1S}\,(\sigma_{1I})$ is the charge density of the zone 1 (in units of e) of a WS cell containing a peptide in binding mode S (I) and a_l is the lipid head group area.

Planar charge density (in units of e) of the zone 2 which basically constitutes the bare membrane reads

$$\sigma_{2i} = -\frac{\alpha_{2i}}{a_l} \tag{3.5}$$

where α_{2i} is the fraction of anionic lipids in the second zone. As described in Eq. 3.3, it is defined based on the binding mode of the peptide at the centre of the cell (i= I, S).

Given the charge density of both regions, we can compute the electrostatic free energy per unit area of each zone using the Poisson-Boltzmann expression for a uniformly charged surface. This electrostatic energy that was already discussed in chapter 2 has the following form

$$F_e(\sigma) = \sigma\,\Psi_0 - \frac{\kappa}{\pi\,l_B}\left[\cosh\left(\frac{\Psi_0}{2}\right) - 1\right] \tag{3.6}$$

with Ψ_0 the electrostatic potential on the surface defined as

$$\Psi_0 = 2\,\sinh^{-1}\left(\frac{2\,\pi\sigma l_B}{\kappa}\right) \tag{3.7}$$

The starting point in our semi-analytical calculations is the total free energy of the WS

cell, F_{ws}, that is written as

$$\begin{aligned}\frac{F_{ws}}{k_BT} &= A_s\,F_e(\sigma_1) + (A_{ws} - A_s)\,F_e(\sigma_2) + \epsilon_I\,\delta_{Ii} \\ &\quad + L_1\Big[\alpha_1\,\ln\alpha_1 + (1-\alpha_1)\,\ln(1-\alpha_1)\Big] \\ &\quad + L_2\Big[\alpha_2\,\ln\alpha_2 + (1-\alpha_2)\,\ln(1-\alpha_2)\Big]. \end{aligned} \tag{3.8}$$

The first two terms describe the electrostatic free energy of the WS cell where the electrostatic charging energy of each zone is given by Eq. (3.6). For WS cells containing a peptide in binding mode I, there is a free energy gain associated with hydrophobic insertion of the peptide, which is denoted by ϵ_I in the third term. This is indeed the parameter that controls hydrophobic binding of peptides in our model. There is a delta function in the third term because for those peptides that are electrically bound to the membrane, *i.e.,* $i = S$, there is no hydrophobic energy contribution to their binding energy. The last two terms account for the entropy contribution of lipid rearrangement around the bound peptide, with L_1 (L_2) the total number of lipids in zone 1 (2).

Note that the entropy of salt ions and their contribution to the electrostatic energy is taken into account in the free energy of the WS cell, F_{ws}, through the charging free energy of each zone, F_e (the relevant discussion is found in Sec. 2.3). Moreover, there is no contribution from the hydrophobic region of the bilayer and charged particles on the other side of the membrane in our free energy. In fact, in our calculations, the interior of the membrane is decoupled from the electrolyte solution, and electric field does not penetrate into the hydrophobic core of the membrane. This assumption is valid as long as $\epsilon_{oil}/\epsilon_w \ll d/\lambda_D$. The thickness of the lipid bilayers, d, is about 40 $\mathring{A}$ and their dielectric constant ϵ_{oil} is around 2. In our system, the membrane is embedded in an electrolyte solution with dielectric constant $\epsilon_w = 80$. The Debye length (λ_D) is taken to be 10 $\mathring{A}$ as it is the typical screening length under physiological conditions. For such choice of parameters the decoupling condition is fulfilled. Thus, we can simplify the calculations by

presuming that there is no interaction between the peptides and salt ions in one side of the membrane and the other ions and charged particles on the other side of the membrane. This is equivalent to treating the membrane as an infinitely thick insulator where we can safely ignore the effect of dielectric discontinuity and the free energy associated with the lipids and ions on the other side of the membrane.

In our mean field scheme, the free energy of a peptide on the membrane is given by the WS cell free energy, F_{ws}, however the adsorption or insertion free energies are calculated with respect to the free energy of the peptide in bulk

$$\mathcal{F} = F_{ws} - F_p \tag{3.9}$$

where F_p is the free energy of the peptide in bulk, which will be described in Sec. 3.3.2. Using the free energy of a WS cell with a peptide in binding mode I (S), we can obtain the corresponding insertion (adsorption) free energy.

Peptides in bulk are modelled as random coils in our approach. Next section is dedicated to this part of our modelling.

3.3.2 Random coil peptides in ionic solutions

Peptides are basically polymers with amino acids as their building blocks, or monomers. However, charged polymers (that is the case for cationic peptides) belong to a specific category of polymers known as *polyelectrolytes*. When dissolved in a polar solution like water, these charged polymers (peptides) adopt a random coil structure basically because of the feasibility of the hydrogen bond formation with water molecules.

The main difference between charged polymers (polyelectrolytes) and neutral polymers is in the electrostatic interactions that are absent in the latter, but play an important role in energetics of the former. In the case of positively charged polymers such as our cationic peptides, the Coulomb repulsion between the charges along the chain tends to expand it. However, this coil expansion is opposed by the entropy that prefers a compact structure with more configurational degrees of freedom. The size of the polyelectrolyte chain is then

determined by the balance of electrostatic interactions and entropy. For polyelectrolytes in an ionic solutions, there is also electrostatic interactions between the back bone charges and the salt ions of the solution. Salt ions promote chain compaction by screening the like charges and thus reducing their electrostatic repulsion. In fact, in the absence of salt ions, highly charged polymers will adopt a fully extended conformation in solution.

Let the polyelectrolyte molecule have N monomeric units each with length b. In the Kuhn formalism of polyelectrolytes that we are going to use here, N is the number of Kuhn segments and b is the Kuhn length. Monomer-monomer interactions in real polymers can be ignored beyond this length [41]. That is, real polymers can be treated like an ideal freely jointed chain if they are considered as a collection of N Kuhn segments each with length b. The polyelectrolyte is carrying a cationic charge Q and is immersed in a (1:1) electrolyte solution with Debye length λ_D.

The free energy of this cationic coil in the ionic solution consists of three main terms: 1) configurational entropy of the chain, 2) attractive interactions between polymer charges and counterions, 3) electrostatic repulsion between the cationic charges on the polymer.

$$F_{coil} = F_{conf} + F_{atr} + F_{rep} \tag{3.10}$$

The configurational entropy of the polyelectrolyte coil is a function of its size which is expressed by the end-to-end distance, R_{ee}, as following [42]

$$F_{conf} = \frac{3}{2}\, k_B T \frac{R_{ee}^{\,2}}{N b^{\,2}} \tag{3.11}$$

where k_B is the Boltzmann constant and T is the temperature.

Electrostatic interactions are computed within Debye-Huckel framework. Following Ref. [43] we use a simplifying assumption to calculate the electrostatic interactions that is more valid at high salt concentrations. For not too low salt concentration where the Debye screening length is small compared to the dimension of the polymer, we can assume that each charge on the chain is surrounded by a cloud of counterions in the form of a sphere of Debye radius. We can now apply the Debye charging method to compute the

electrostatic interaction of charges with their surrounding counterions. In other words, we charge up our polymer in the ionic solution to its final charge Q and calculate the corresponding charging free energy. Note that the salt ions in the ionic solution are not involved in the charging process. As polymer is charging, the counterion spheres, which are also called ionic atmospheres in the DH theory, are formed around the back bone ions [44]. The free energy related to the formation of each ionic atmosphere is indeed the Debye charging energy of a point charge in an ionic solution which is known in the DH theory [45]. Therefore, the second term in the free energy of the coil F_{coil} is given as

$$F_{atr} = -\frac{Q\,\kappa\,e^2}{8\pi\epsilon_0\epsilon_w} \tag{3.12}$$

where κ is in the inverse of Debye length, e the elementary charge and ϵ_w the dielectric constant of the salt solution. This free energy in units of k_BT can be written as a function of Bjerrum lengh $l_B = e^2/(4\pi\epsilon_0\epsilon_w k_BT)$ as following $F_{atr}/k_BT = -Q\,\kappa\,l_B/2$.

The repulsive interactions between backbone charges are now screened due to the presence of the ion atmospheres. These intrachain interactions are calculated for a fixed end-to-end distance. Let us consider the i-th and j-th charge on the polyelectrolyte that are m segments apart along the chain. Within the DH theory, their repulsive energy is given as

$$\frac{u_{ij}}{k_BT} = \frac{l_B \exp\left(-\kappa\, r_{ij}\right)}{r_{ij}} \tag{3.13}$$

where r_{ij} is the variable distance between the charges dependent on the molecular configuration. However, for any two pair of charges on the polymer we should take an average on all the possible values of r to find their average interaction energy

$$\bar{u}_{ij} = \int_0^\infty W(r; R_{ee}, m) u_{ij} dr \tag{3.14}$$

with $W(r; R_{ee}, m)$ the distribution function for the probability of having a distance r between two charges that are m Kuhn segments apart along a chain with end-to-end distance R_{ee}. The total repulsive energy of the polyelectrolyte is now obtained by summing

up the contributions from all possible pair of charges (the detailed derivation can be found in Ref. [43]). Thus, the last term in F_{coil} is written as

$$\frac{F_{rep}}{k_B T} = \frac{Q^2\, l_B}{R_{ee}} \ln\left(1 + \frac{6R_{ee}}{\kappa N b^2}\right) \tag{3.15}$$

Including all the three contributions, the total free energy of the charged coil per units of $k_B T$ is

$$\frac{F_{coil}(R_{ee})}{k_B T} = \frac{3}{2}\frac{R_{ee}^{\,2}}{N b^{\,2}} - \frac{Q\,\kappa\, l_B}{2} + \frac{Q^2\, l_B}{R_{ee}} \ln\left(1 + \frac{6R_{ee}}{\kappa N b^2}\right) \tag{3.16}$$

This energy is just a function of polymer end-to-end distance, R_{ee}. The equilibrium size of the polymer (given by $R_{ee}^{\,eq}$) is found by minimization of the free energy in Eq. 3.16 with respect to $R_{\,ee}$. The free energy of the polymer at equilibrium will then be $F_{coil}(R_{ee}^{\,eq})$ which is indeed the peptide free energy in bulk F_p that we have used in Eq. 3.9

3.3.3 Total free energy of the peptide-membrane system

So far we have calculated the electrostatic free energy of a WS cell containing a peptide, as well as the free energy of a peptide in bulk, however peptide binding is associated with some other effects that are not included in the WSC energy in Eq. 3.8. One of these effects that does not depend on the electrostatic interactions is the mechanical deformation of the membrane induced by bound peptides. In our approach, peptides in binding state S that are just adsorbed to the head group of lipids, unlike those that bind to the interface, do not induce any mechanical deformation to the membrane. Peptides in binding state I that are inserted at the interface between the head group of lipids and their hydrocarbon chains will then introduce an extra area to the interface, $\mathcal{A}_P$, which is concomitant with a local deformation in the membrane. When bound to the interface, the peptides push the lipids away and form gaps underneath in the hydrocarbon core of the membrane (see Fig. 3.1). Lipid tails bend toward the hydrophobic side of the peptide to fill the gap, and consequently there is a local membrane thinning and bending. The corresponding range of local deformations has been estimated to be $\xi = (16\, h^2\, K_C/K_A)^{1/4}$ where h is the

hydrocarbon thickness of the lipid bilayer, K_C the bending modulus and K_A the stretch modulus [46]. If peptide spacing (distance between bound peptides that is $2R$ in our model) is smaller than the range of deformations (ξ), the local deformations by individual peptides on the membrane overlap. In this limit, the membrane thickness decreases almost uniformly or equivalently the membrane area increases almost uniformly.

In our calculations, we assume the uniform membrane deformation induced by peptide binding, which is justified by the high concentration of peptides on the membrane. Introducing $\mathcal{A}_P$ as the area increase due to binding of one peptide in the I state, the fractional area stretch in the membrane is then written as $\Delta A/A = \sigma_I \mathcal{A}_P$. The area expansion induces a stress to the membrane similar to that of an external tensile force. In fact, the peptide-mediated area expansion could be considered as a tension on the membrane [21, 20]. The peptide-induced tension on the membrane is sometimes called an internal tension, simply because it is not due to an external force [46]. Analogous to an external tension the internal tension in the membrane is defined as $\tau = K_A \Delta A/A = K_A \sigma_I \mathcal{A}_P$ [21]. The relevant deformation energy per unit area of the membrane is then written as $F_{stretch}/A = 1/2\,\tau \Delta A/A = 1/2 K_A (\sigma_I \mathcal{A}_P)^2$. This elastic energy contribution is also going to be included in the total free energy of our membrane-peptide system.

Including all the effects, the total free energy change of the peptide-lipid system upon binding, per unit area, is expressed as,

$$\begin{aligned}
\frac{\Delta F}{k_B T} &= \sigma_I \mathcal{F}_I + \sigma_S \mathcal{F}_S + \frac{1}{2} K_A (\sigma_I \mathcal{A}_P)^2 \\
&\quad + \left[\sigma_I \ln(\sigma_I A_p) + \sigma_S \ln(\sigma_S A_p) + (\sigma_M - \sigma_I - \sigma_S) \ln\left(1 - \frac{\sigma_I + \sigma_S}{\sigma_M}\right) \right] \\
&\quad + \frac{1}{N_t A} \Big[\big(N_p - N_t A (\sigma_I + \sigma_S)\big) \ln\Big[\big(N_p - N_t A (\sigma_I + \sigma_S)\big) v_p / V \Big] \\
&\quad - \big(N_p - N_t A (\sigma_I + \sigma_S)\big) \Big] - F_{ref}
\end{aligned} \tag{3.17}$$

where F_{ref}, the free energy of the reference state, is written as

$$F_{ref} = F_e(\sigma_0) + \frac{1}{a_l}\Big[\bar{\alpha}\,\ln\bar{\alpha} + (1-\bar{\alpha})\,\ln(1-\bar{\alpha})\Big] + \frac{1}{N_t A}\Big[\,N_p\,\ln\Big(\frac{N_p\,v_p}{V}\Big) - N_p\Big] \qquad (3.18)$$

The first two terms in Eq. 3.17 give the total charging free energy per unit area of the membrane covered by bound peptides; σ_I and σ_S are the planar density of the peptides in surface adsorbed and inserted state, respectively, and $\mathcal{F}_I(\mathcal{F}_S)$ the insertion (adsorption) free energy defined in Eq. 3.9. The third term describes the membrane elastic energy that is basically the energy cost for peptide insertion. In this term, K_A is the area stretch modulus of the bilayer, and $\mathcal{A}_P$ the area expansion per each peptide in binding mode I, which is equal to A_p or $A_p/2$ for the symmetric and asymmetric peptide binding, respectively (this is discussed in detail in Sec. 3.4.2). In the fourth term, translational entropy of the bound peptides is expressed through a two-dimensional lattice model where, A_p is the area occupied by a bound peptide and $\sigma_M = 1/A_p$ the planar density of binding sites for peptides on the membrane. The fifth term accounts for the configurational entropy contribution of free peptides to the free energy; here N_t is the total number of target cells (either host cell or bacterium), A the area of each target, N_p the total number of peptides in the peptide-lipid system, V the total volume, and v_p the volume of a peptide in bulk.

In order to calculate the entropy of peptides in bulk we have used a 3D lattice model similar to the one used for peptides on the membrane. Furthermore, we have considered a dilute solution of peptides in bulk, since the concentration of peptides is typically low in the solution ($\sim \mu M$) [33]. Entropy of the solutes in a dilute solution has the well-known form of $S/k_BT = N\ln(c) - N$ with N the total number of solutes and c their volume fraction in the solution. Applying the same entropy to our peptides in the electrolyte solution, N would be the total number of free peptides and c the volume fraction of free peptides in bulk, that is the total volume occupied by peptides in bulk/total volume of the system. When the solution is not connected to a peptide reservoir similar to our system, the number of free peptide and subsequently their volume fractions is not conserved. Binding of peptides to the targets will reduce the number of free peptides in the solution. In our approach, the total number of bound peptides in equilibrium is expressed as $N_t A\,(\sigma_I + \sigma_S)$ where $\sigma_I(\sigma_S)$ is

the equilibrium density of peptides in binding mode I(S) on the cell membranes. Therefore, the number of peptides that remain free in the solution would be $N_{free} = N_p - N_t A\,(\sigma_I + \sigma_S)$ with N_p the total number of peptides in the system.

In Eq. 3.17, the reference energy is subtracted from the total free energy of the system to give us ΔF. In our approach, the reference state is assumed to be the one in which there are no peptides on the membranes, *i.e.,* all the peptides are free in bulk. In the free energy of the reference state defined in Eq. 3.18, the first term is the electrostatic free energy of the bare membrane that is treated like a flat surface carrying a uniform charge density of $\sigma_0 = -\bar{\alpha}/a_l$ (in units of e). Electrostatic free energy of this charged surface denoted by $F_e(\sigma_0)$ follows Eq. 3.6. The second term gives the translational entropy associated to the lipid mixture of the membrane, with $\bar{\alpha}$ fraction of anionic lipids to neutral ones. The last term accounts for the entropy of the peptides which are all free in the ionic solution in the reference state. Note that electrostatic energy of each peptide in the reference state is already included in the adsorption and insertion energies, $\mathcal{F}_S$ and $\mathcal{F}_I$, respectively, in Eq. 3.17.

Note that in our approach, as seen in the Eq. 3.17, there is no interaction between the target cells. Furthermore, different types of cells are considered separately (*i.e.,* all the cells in the solution are similar and, for instance, carry the same fraction of anionic lipids $\bar{\alpha}$).

The total free energy of the peptide-membrane system in our model, Eq. 3.17, is actually a function of four independent variables, σ_I, σ_S, α_{1I} and α_{1S}. The equilibrium value of these variables is found by minimization of the free energy, which was accomplished using the MATLAB's optimization toolbox: FMINCON and FMINSEARCH functions.

3.4 Results and Discussions

3.4.1 Binding isotherms

Minimization of the free energy gives us the equilibrium density of the peptides on the membrane in different binding modes, *i.e.,* σ_I, σ_S. However our main focus is on the peptides in binding mode I that have a major effect in membrane perturbation. More particularly, we calculate the surface coverage of peptides inserted into the interface between the lipid head groups and their tails that is denoted by P/L and is defined as the total number of peptides in binding mode I divided to the total number of lipids on the membrane.

In our calculations, the parameters of the peptide-membrane system are chosen as follows. Independent of the type of the membrane and peptide, we always have T = 300 K, V = 1L, $K_A = 0.578\, k_BT/\mathring{A}^2$, $\lambda_D = 10\,\mathring{A}$, and $\epsilon_w = 80$. For the peptide parameters, we have used the typical values for Melittin which is a well characterized antimicrobial peptide with Q = 6, and $\epsilon_I = -14\, k_BT$. The volume of the peptides in bulk is given by the size of the random coils (Sec. 3.3.2) as $v_p = {R_{ee}}^3 = 33^3 \mathring{A}^3$.

Two different sets of parameters have been used for the membranes, corresponding to two different types of target cells. To mimic the bacterial membrane we use $\bar{\alpha} = 0.3$ (a typical value for a bacterial membrane), $a_l = 71$, and $A_p = 162$, and for the host cell membrane we have $\bar{\alpha} = 0.05$, $a_l = 74$, and $A_p = 246$. The values of a_l and A_p are taken from Ref. [22], where the interaction of Melittin with model membranes was considered. In the bacterial membrane, the average headgroup area of lipids is smaller than that of the host cells due to abundance of PE (Phosphatidylethanolamine), which is the principle phospholipid in bacterial membrane [24] and has a smaller headgroup than PC (phosphatidylcholine) [47] the principle lipid in the membrane of host cells. The different values of A_p (the area occupied by peptide on the membrane) for different targets is justified by the dehydration effect [22]. Normally the polar headgroup of lipids are surrounded by water molecules which are not tightly bound and are released from the headgroup region when a peptide is embedded in the membrane. Thus the area occupied by the peptide on the membrane is related to this dehydration effect: the more enhanced dehydration results

in the smaller area occupied by the bound peptide. In the bacterial membrane with smaller lipid headgroup area, more water molecules are released by peptide binding, which leads to a smaller value for A_p.

Cationic antimicrobial peptides are known to use the compositional difference between bacterial and host cell membranes to discriminate between them [10, 12]. In the plasma membrane of bacteria, which is the main target of AMPs, the outer layer is abundant in anionic lipids whereas in the plasma membrane of host cells, most of the anionic lipids are in the inner layer facing the interior of the cell. Accordingly, stronger electrostatic attraction between cationic peptide and negatively charged membrane of bacteria helps them to differentiate between host cells and bacteria in order to kill the right one. We have also considered different surface charge densities for the two types of membranes modelled here. In the bacterial mimicking membrane, thirty percent of the lipids are negatively charged *i.e.*, $\bar{\alpha} = 0.3$ and the host cell- mimicking membrane carries a number of anionic lipid ($\bar{\alpha} = 0.05$) that yield a weak negative surface charge density [9]. As the first step to investigate the antimicrobial activity and selectivity of Melittin, we have considered its binding isotherms on different membranes as shown in Fig. 3.5. The molar ratio of membrane-perturbing peptides in binding mode I to lipids, P/L, is higher on the bacterial membrane than on the host cell membrane which indeed reveals the selective membrane-disruption activity of the peptide. Here, we have chosen the target cell density to be $C_t = 5 \times 10^5\, cells/mL$ which is a typical cell density in bacterial assays [8], however, peptide selectivity can be shown for other target densities as well.

To investigate the effect of cell density on peptide binding, as one of the main goals of this thesis, we have produced binding isotherms for a range of cell densities which are consistent with those used in the relevant experimental works [8]. Fig. 3.6 and Fig. 3.7 illustrate our results for the bacterial and host cases, respectively. For any target density, at very large concentration of peptides in bulk, *i.e.,* $C_p \gg C_t$, binding isotherms converge to that of a single target case . Indeed, when there are lots of peptides in the solution, binding on one cell membrane is not affected by the presence of other cells as if we just had one single membrane. However, if we decrease the concentration of peptides in the solution, at some point cells start to 'see' each other, that is binding on one cell diminishes

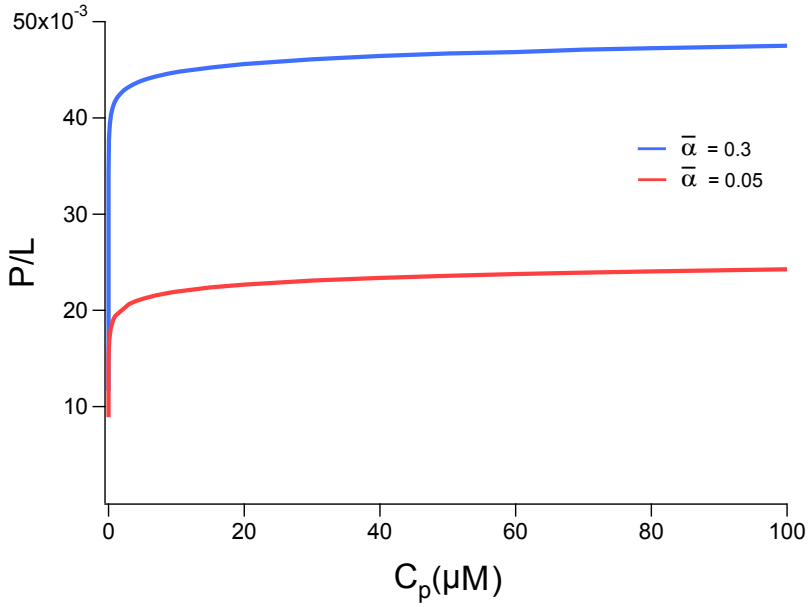

Figure 3.5: The molar ratio of membrane-embedded peptides (in binding mode I) P/L, a good measure of membrane perturbing activity of AMPs, as a function of concentration of peptides in bulk C_p for peptide charge $Q = 6$. Higher binding of peptides on the bacterial membrane with $\bar{\alpha} = 0.3$ compare to that of the host cell with $\bar{\alpha} = 0.05$ is seen in this figure, which reflects the selective antimicrobial activity of the peptide.

the amount of free peptides for other cells, and thus binding is lowered sharply and goes to zero for small peptide concentrations.

The effect of cell density on peptide binding is better seen when we fix the peptide concentration and change the density of target cells . The result is separately displayed in Fig. 3.8. Our model shows that concentration of target cells C_t does affect peptide binding. According to our free energy formalism, Eq. 3.17, this is an entropic effect which is seen if the total number of peptides is fixed in the system. In fact, target density affects peptide binding by influencing the amount of free peptides. Introducing a density of cells to the solution is equivalent to reducing the number of "available" free peptides for each cell; there is a 'competition' between cells to attract peptides, recalling that the total number of peptides is fixed in the solution. Due to this competition, the molar ratio of bound peptides to lipids on the membrane P/L is lower in a multi-target system than in a single-

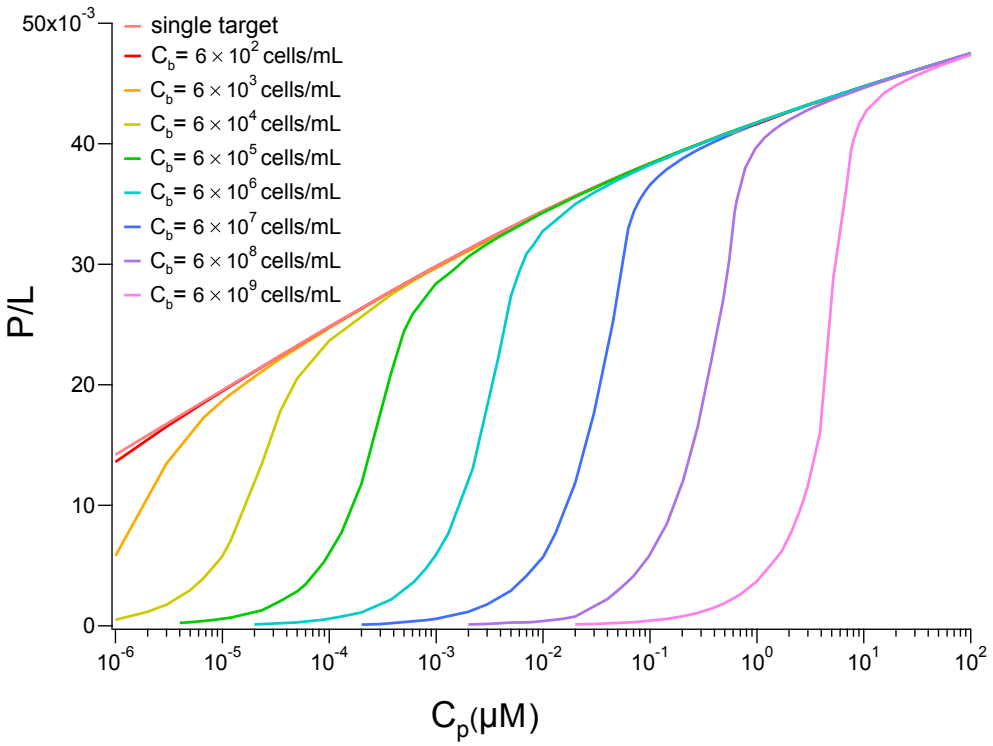

Figure 3.6: The molar ratio of the membrane-disrupting peptides (in binding mode I) to lipids P/L as a function of peptide concentration in bulk C_p, for $\bar{\alpha} = 0.3$ (typical for a bacterial membrane), peptide charge $Q = 6$ and various bacterial cell densities C_b as specified in the figure. By increasing the cell density, binding starts at a higher peptide concentration. The binding isotherm of the single target case (one cell in the solution) is also included for comparison. For any cell density, at very high peptide concentration when $C_p \gg C_b$, binding follows the behaviour of the single target case.

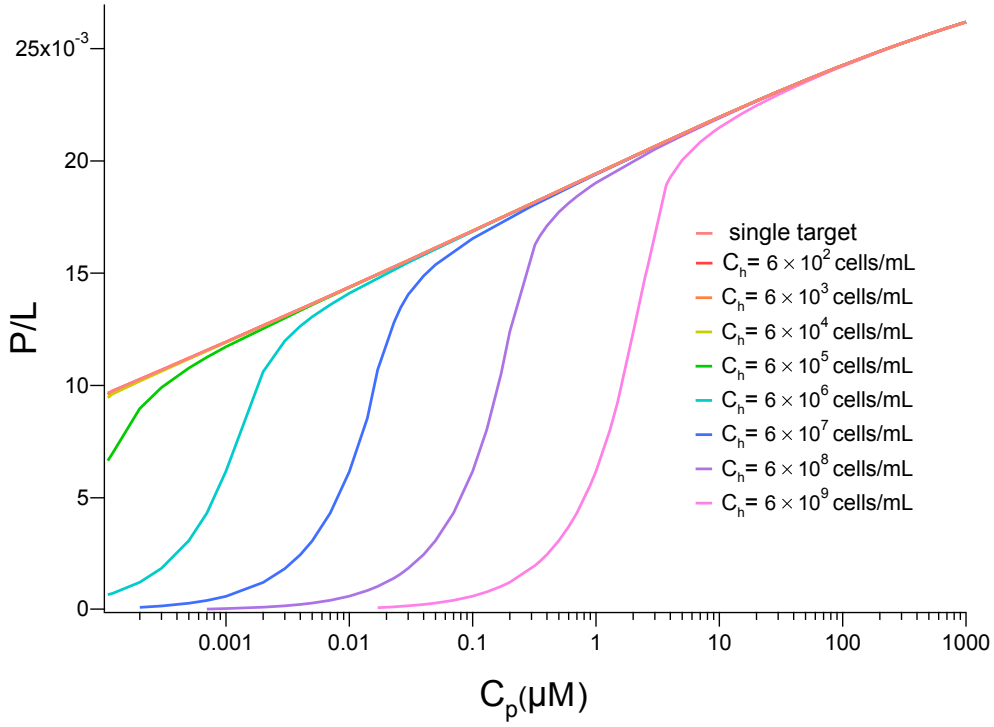

Figure 3.7: P/L as a function of peptide concentration in bulk C_p, for the host cell membrane $\bar{\alpha} = 0.05$, peptide charge $Q = 6$ and various host cell densities C_h as specified in the figure. Similar to the bacterial membrane case: by increasing the cell density, binding starts at a higher peptide concentration. The binding isotherm of the single target case (one host cell in the solution) is also included. For the first three choices of the cell density, binding is similar to the single target cell (plots lie on top of each other). Nevertheless, binding isotherms of all the cell concentrations, in general, converge to that of the single cell case at high concentrations of peptides.

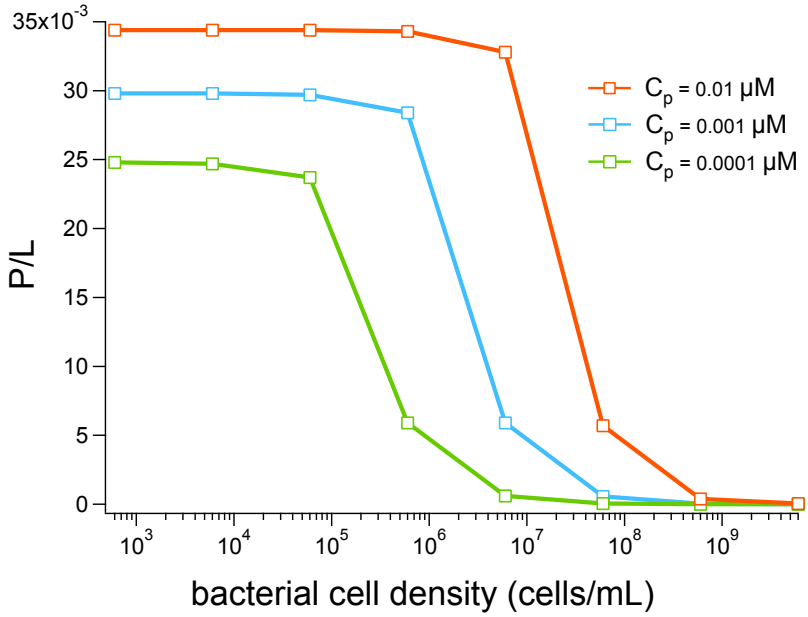

Figure 3.8: P/L as a function of cell density for the bacterial case ($\bar{\alpha} = 0.3$) and a few choices of bulk peptide concentration C_p. For a fixed C_p, binding is constant at very low cell densities, it then decreases by increasing the cell density and goes to zero for very large densities of bacterial cells. However, the cell concentration at which binding is diminished is higher for a larger value of C_p.

target one. At very low densities ($C_t \ll C_p$), however, there is no competition between cells and binding on target cells does not significantly reduce the number of free peptides in bulk. Thus, P/L does not change by cell density and is equal to that of a single target case exposed to C_p concentration of peptides in solution. Nevertheless, by increasing the number of cells, at some density they start to see each other, which is where the inter-cell competition starts. Subsequently, peptide binding is decreased by increasing the cell densities and ultimately goes to zero at very high densities of target cells. As seen in the Fig. 3.8, the onset of peptide binding attenuation depends on the bulk concentration of peptide; It occurs at a higher cell density, for larger values of bulk peptide concentration. In addition, as expected, for a fixed cell density, the larger the C_p the higher the P/L would be.

3.4.2 Asymmetric binding of peptides

When electrostatically attracted to the membrane, peptides first bind to the outer leaflet of the lipid bilayer. However, their amphiphilicity allows them to have hydrophobic interaction with the core of the membrane, which indeed facilitates translocation of the bound peptides to the inner leaflet of the bilayer and if finally, peptide distribution will be symmetrized between the two leaflets [48, 24]. Our calculations so far correspond to this extreme symmetric binding of peptides, which is usually the case in experimental works that study stacks of parallel lipid bilayers with bound peptides [22]. However, we have also attempted to make binding isotherms related to the initial asymmetric binding of peptides on the membrane to see how symmetrization influences peptide activity.

In order to simulate the asymmetric binding of peptides, we needed to make some changes to our model. We believe that the elastic energy of the membrane is defined differently based on the symmetry of peptide binding. In asymmetric binding, there are no peptides in the inner layer and all the peptides bind to the outer layer. In this case, the mechanical deformation of the membrane induced by peptide binding is shared between the two monolayers which is explained as follows. Insertion of peptides at the interface between lipid headgroups and tails stretches the membrane, however in the asymmetric binding, this will be accompanied by the expansion of lipids in the inner layer as well. This energetically unfavourable lipid expansion in the inner layer is balanced with the compression of lipids in the outer layer such that, in the end, the membrane area is stretched by $A_P/2$ per inserted peptide. Accordingly, the mechanical deformation term in the free energy of the system would be altered as $1/2\, K_A\, (\sigma_I A_p/2)^2$. This is indeed analogous to a one dimensional system of two identical parallel springs each with length x_0 which are coupled to each other such that any compression or expansion in one them will directly affect the length of the other one too. Now if an object of length L is added to one of them, the final stretched length of the two strings will be $x = x_0 + L/2$.

By conserving the total number of lipids, the reduced area per lipids in the outer layer is estimated to be $a_l' = a_l\,(1 - \sigma_I\, A_p/2)$. Therefore, in asymmetric binding analysis, we will use this shrunk headgroup area instead of a_l in our free energy in Eq. 3.17. Note that

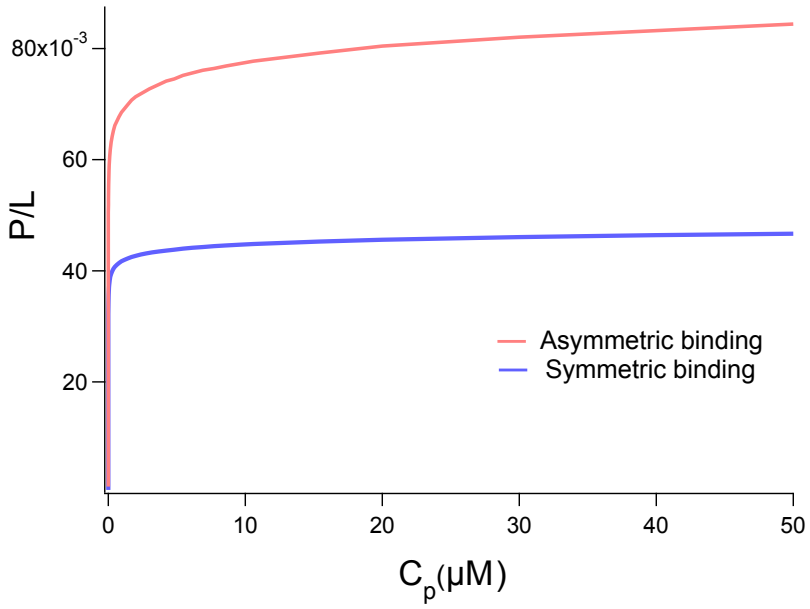

Figure 3.9: P/L as a function of bulk concentration of peptides C_p, for peptide charge Q = 6, $\bar{\alpha} = 0.3$ and $C_t = 5 \times 10^5$ cells/mL. In the symmetric binding, there are less number of peptides to lipids on the outer layer, compared to the asymmetric case.

we always consider binding of peptides on the outer layer (although it is not an issue in symmetric binding, because peptide concentration is the same on both layers).

In addition, since peptides just bind on the outer layer in the asymmetric binding, the total number of peptide binding sites on the membrane is half of those in the symmetric binding. Accordingly, the membrane area A will be altered to $A/2$ in the asymmetric binding. Plugging all the aforementioned changes to the free energy of the peptide-membrane-solution system in Eq. 3.17, and minimizing it (similar to what we did for the symmetric binding), we have made binding isotherms for the asymmetric binding of Melittin on the membranes. Fig. 3.9 shows our results. In the symmetric binding case, distribution of peptides between the two monolayers along with a higher elastic energy of the membrane results in a lower number of bound peptides to lipids, P/L, in the outer layer compared with the asymmetric binding of peptides. In both cases, however, P/L is saturated for large concentrations of peptides in bulk. The saturation value in the asymmetric binding is almost twice as much as in the symmetric one.

3.4.3 Peptide selectivity: therapeutic index

The main feature of antimicrobial peptides is that they selectively rupture the membrane of bacteria over that of host cells. In this section we consider the effect of target concentration on peptide selectivity or more specifically on the peptide therapeutic index.

Therapeutic index is a good measure of peptide selectivity which is defined as MHC/MIC where MHC is the minimum haemolytic concentration of the peptide for the host cells and MIC its minimum inhibitory concentration for the bacteria. MIC and MHC are, in fact, the bulk concentrations of the peptides at which they effectively rupture the membrane of bacteria and host cells, respectively.

It has been observed in experiments that AMPs are inactive against their targets below a threshold concentration on target membranes, which we denote by P/L^* [20, 22]. In other words, for P/L below P/L^* no pore was observed on the membrane, but as P/L exceeds P/L^* transmembrane pores appeared on the membrane [22]. Thus, there seems to be a correspondence between the two critical peptide concentrations described as follows [33]. Regarding the antibacterial activity of the peptides, if the total concentration of the peptides in solution is around MIC, (*i.e.,* $C_p \approx$ MIC), the concentration of the peptides on the membrane is close to the threshold concentration, that is $P/L \approx P/L^*$, and a similar thing applies when the targets are host cells for which MIC is substituted by MHC.

In what follows, we use our binding isotherms and the aforestated relation between the threshold concentrations of the peptides to calculate their therapeutic index. Given the P/L^* for bacteria and host cells, we can exploit our results in figures 3.6 and 3.7 to extract the corresponding peptide concentration in bulk which is MIC or MHC respectively, and thus compute its therapeutic index. However, the question is now how should we select P/L^* for different targets? More particularly, is the peptide threshold surface coverage required for rupture the same for the membrane of bacterial and host cells?

To answer this question, we should figure out if the the lipid compositional differences between the membrane of bacteria and host cells can affect the threshold rupture concentration of the peptide P/L^*.

3.4.4 Lipid packing shape and threshold surface coverage

A universal characteristic of membrane-lytic antimicrobial peptides is their cooperativity that is independent of their mode of action, a threshold concentration P/L^* is required for their activity below which no significant effect can be seen [20, 33]. They are, therefore, said to disrupt the membrane in a so called all-or-none concentration dependence manner [16].

On the correlation between the peptide critical concentration P/L^* and lipid composition, our first question was how do charge properties of the membrane affect the rupture concentration of peptides? The answer of this question was found in the work of Weiprecht, *et al.* [49]. They studied the interaction of the cationic peptide PGLa with neutral and negatively charged model membranes and showed that membrane charge will just affect the initial binding of the peptides. In fact, by excluding the electrostatic interactions and focusing on the surface concentration of the peptides instead of their bulk concentrations, they obtained the same threshold concentrations for peptides on both anionic and neutral membranes. Thus, it appears that P/L^* does not depend on the charge of the membrane.

Nevertheless, Huang did more systematic analysis to explore the lipid dependence of collective activities of AMPs. His group studied the interaction of different AMPs with model membranes of various lipid compositions and measured the threshold P/L^* of the peptides via different experimental methods [22, 21]. Their measurements showed that the peptide concentration required for membrane rupture P/L^* does depend on the lipid composition of the membrane. More specifically, they studied model membranes with different concentrations of positively curved lipids (lysoPC) or negatively curved ones (PE) and observed that peptide threshold concentration P/L^* is larger for membranes consisting of higher amounts of negatively curved lipids (lipid curvature was described in Sec. 1.3) [22]. This was consistent with the earlier observations where addition of PE inhibited formation of toroidal pores by magainin and melittin while addition of lysoPC facilitated their formation [26, 19]. The idea was that lipid curvature correlates with the curvature of the pore, and thus formation of toroidal pores with a mean positive curvature is facilitated by lipids of positive curvature (lysoPC) and is prevented by lipids of negative curvature

(PE). However, Huang *et al.* observed the same lipid dependence for both melittin (with toroidal pores) and alamethicin (with barrel-stave pores) systems [22]. This interesting observation therefore shows that the effect of lipid curvature on pore formation must be through something other than the pore curvature because alamethicine pores are known to have a zero curvature.

Based on the large extent of research on the widely studied AMPs alamethicin, melittin, magianin and protegrin, Huang proposed a two-state model to explain the collective antimicrobial activity of peptides which indeed enabled him to clarify the lipid dependence of P/L^* as well [20].

According to his model, there are two binding states for peptides on the membrane: surface state S with energy level $-E_S$ and pore state P with energy level $-E_p$, where, in general $E_S > E_p$ (*i.e.,* the surface state is more stable than the pore state) [20]. Not to be confused with our binding model of peptides, the surface state here refers to the membrane perturbing peptides (equivalent to our binding mode I). In fact, surface adsorbed peptides are not considered in this model since they have a minor impact on membrane perturbation. When the concentration of peptides is below the threshold concentration, all the bound peptides occupy the surface state where they are embedded in the membrane and concomitantly increase the membrane area. This energetically unfavourable membrane area stretch is assumed to be equivalent to a membrane tension that scales with P/L. Therefore, a positive term which increases with P/L is added to the energy level of the S state. Peptide binding then increases the energy level of the S state and eventually, once the concentration of the peptides on the surface reaches the threshold P/L^*, the energy level of surface state becomes higher than that of the pore state. Consequently for P/L above P/L^*, all the excessive peptides will directly go to the pore state, that now has a lower energy than the S state, and contribute to pore formation.

Within his two-state model, Huang has obtained the threshold concentration as $P/L^* = (E_S - E_P)/K_A(A_p^2/a_l)(1-\beta)$, where K_A is the area stretch modulus of the lipid bilayer, A_p the membrane area expansion per bound peptide (in the S state), a_l the area of the lipid headgroup and β is a parameter that determines the contribution of pores in the membrane thickness [20, 22]. Measuring all the above experimental parameters related to P/L^* and

analysing the data, his group eventually found the underlying reason of lipid dependence of P/L^*. Regardless of the type of peptide, a strong correlation was observed between the variations of P/L^* and the membrane thinning effect quantified by A_p [22]. The smaller the A_p, the larger the threshold concentration P/L^* is for both type of pores. Thus, A_p is a dominant factor in determining the lipid dependence of P/L^*.

Membrane thinning measurements for various peptide-lipid systems show that A_p strongly depends on the lipid composition. It is smaller in membranes with higher amounts of negatively curved lipids [22]. As a result, the higher the concentration of lipids of negative curvature in the membrane, the larger number of peptides are required for membrane disruption (a larger P/L^*).

The lipid dependence of A_p is believed to be due to the lipid dehydration effect of peptide binding. When peptides bind to the membrane, some water molecules are released from the headgroup region of lipids and thus reduce the area expansion by the peptides. For negatively curved lipids, where their headgroups have a smaller cross sectional area than their hydrocarbon chains such as PE (see Sec. 1.3), there are more water molecules surrounding the headgroups compare to positively curved lipids. Therefore, more water molecules are released from the headgroup of negatively curved lipids by peptide binding than from the positively curved ones. Consequently addition of PE to the membrane decrease A_p whereas addition of LysoPC (a positively curved lipid) increases it [22].

Huang *et al.* studies indeed shed light on a universal effect of lipid spontaneous curvature on the pore formation activity of AMPs. During their extensive studies on AMPs, they also measured significant parameters of various peptide-lipid systems that are related to pore formation. We have also used some of their melittin-lipid parameters in this thesis.

We can now answer the question about the difference between the threshold concentration of AMPs on the host cells and bacterial membrane. According to the universal curvature effect of lipids and the fact that PE (with negative curvature) is the principal phospholipid in bacteria while in the host cells PC (with zero curvature) is the main lipid constitution, we conclude that the threshold peptide concentration P/L^* is larger for the bacterial membranes than host cells.

In our model, we have implicitly captured the lipid curvature difference between the membranes of host cells and bacteria through a parameter, A_p, that represents the area occupied on the membrane by bound peptides. The degree of membrane mechanical deformation induced by peptide binding is also quantified by A_p, in our approach. The membranes of bacteria are rich in PE while the host cell membranes are abundant in PC, thus according to the curvature effect of lipids, peptides are better accommodated in the former. We have taken into account this difference by choosing a smaller A_p on the membrane of bacteria than that of host cells.

Huang's group has measured P/L^* of the Melittin on PC and PC/PE model membranes [22] that are the commonly-used lipid compositions to mimic the host cell and bacterial membrane, respectively. Using their experimental parameters, we take the threshold concentration of Melittin to be $P/L^* = 1/48$ on the bacterial membrane and $P/L^* = 1/99$ on the host cell membrane [22].

Given the threshold concentration P/L^* of the peptide on the membrane, we can now use our binding isotherms, as shown in the Fig. 3.10, to extract the corresponding bulk values which are indeed MHC and MIC.

Doing the binding calculations for varying cell densities enabled us to elicit MIC and MHC for different cell densities. Fig. 3.11 depicts our results for MIC and MHC as a function of cell density. Both MHC and MIC increase with increasing cell density. This concentration-dependence activity of AMP can be understood as follows: since the total number of peptides is conserved, peptide biding is influenced by cell density. The higher the cell density, the fewer bound peptides (this was already shown in Fig. 3.8, and the relevant discussion is found in the Sec. 3.4.1). Therefore, at a higher cell density, more peptides in bulk will be required in order for P/L to reach the threshold value P/L^* for membrane disruption. Consequently, MIC and MHC are higher at higher cell densities.

For minimum hemolytic concentration MHC, we considered two different cases: (1) host cells have the same area as the bacteria, (2) area of the host cells, A_H, is larger than that of the bacteria,A_B, by a factor of 17. In the first case, we have chosen the target areas as $A_H = A_B = 12 \times 10^{-12} m^2$, which is twice the surface area of E. *coli*. The factor two

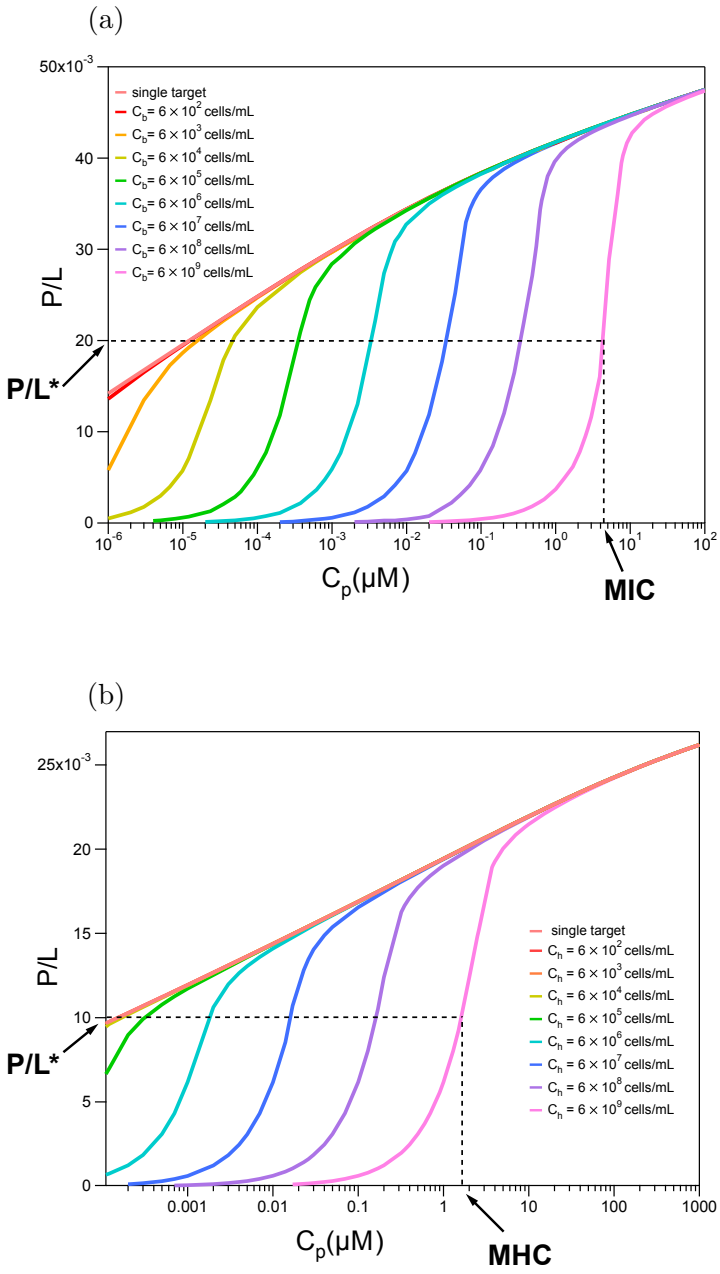

Figure 3.10: (a) Extraction of MIC for peptide charge Q = 6 and various densities of bacteria. (b) Extraction of MHC for various densities of host cells and peptide charge Q = 6. In both cases, we have used the experimental data for P/L^*.

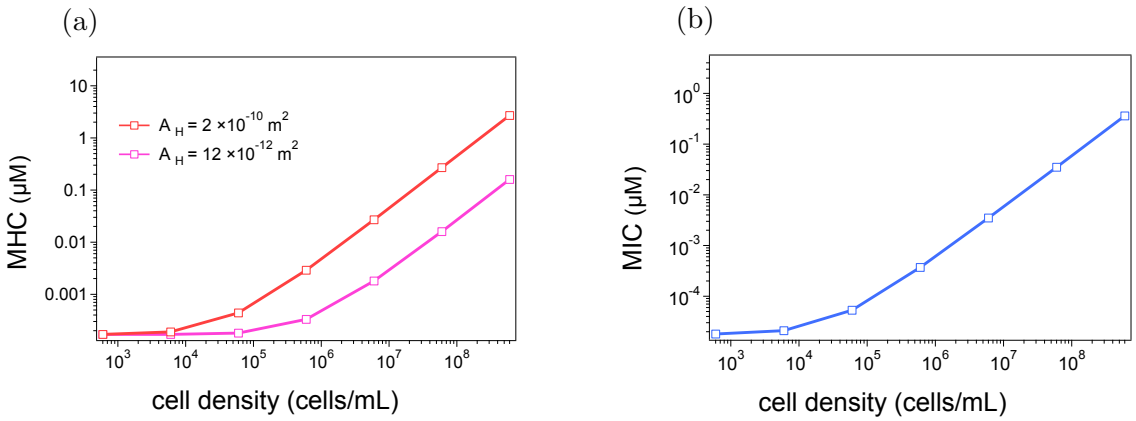

Figure 3.11: (a) MHC as a function of cell density for peptide charge $Q = 6$ and two choices of cell area as specified in the figure. (b) MIC as a function of cell density for $Q = 6$ and target membrane area $A_B = 12 \times 10^{-12}$.

is needed for the symmetric binding of peptides on the membrane, because peptides bind onto both leaflets of the lipid bilayer. However, in reality host cells (red blood cells) are larger than bacteria. The surface area of a red blood cell is of the order of $10^{-10}m^2$. Thus, we did calculations for a more realistic situation as well, where $A_H = 17\,A_B$. Fig. 3.11 shows MHC as a function of cell density for the two different choices of cell area.

MHC increases by increasing the host cell area for the same reason as it increases by increasing the cell density. In fact, in our multi-target analysis, increasing either of the cell surface area or number of the cells increases the total number of peptide binding sites (given by $N_t A$), and thus produces the same effect. In principle, in our model (see Eq. 3.17) we can combine these two parameters into just one parameter which is equivalent to reducing our multi-cell system to a single cell with a large area of $\mathcal{A} = N_t A$. Therefore, increasing the cell area has the same effect in our calculations as increasing the cell density. Thus, in our area basis analysis, instead of increasing the area we can increase the cell densities accordingly. More specifically, in Fig. 3.11, we can obtain either of our MHC curves from the other one by rescaling the x axis (cell densities).

Using the results for MHC and MIC, it is now possible to investigate the effect of cell

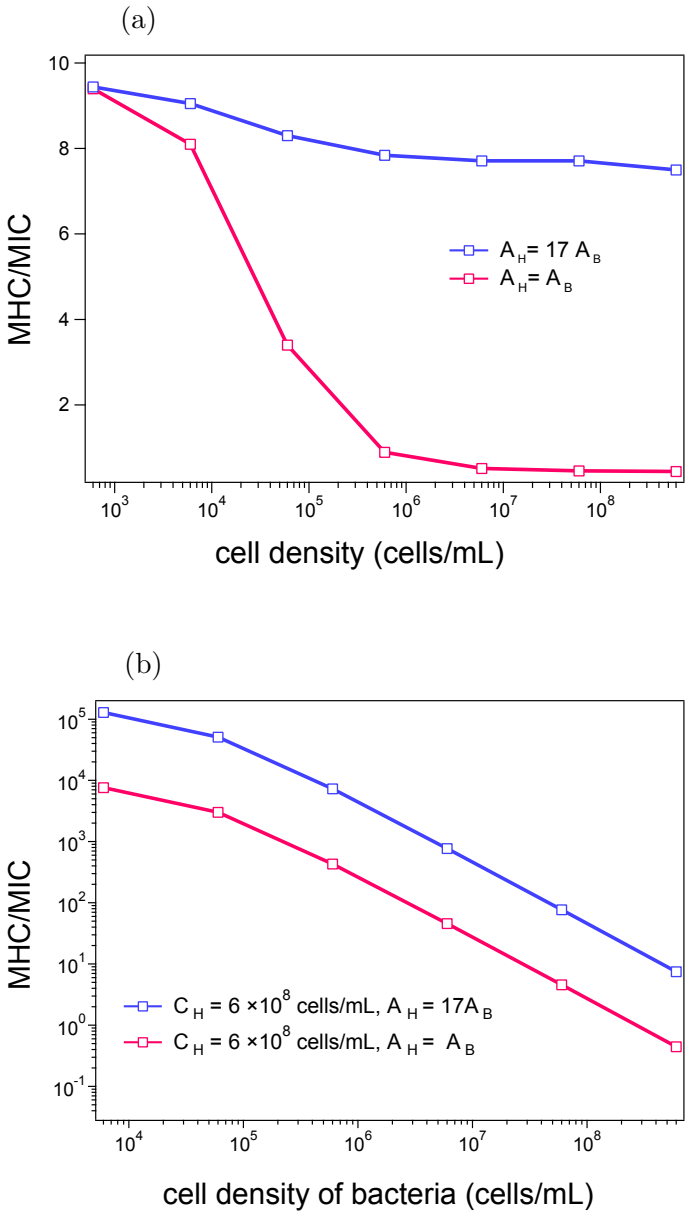

Figure 3.12: MHC/MIC, a good measure of peptide selectivity, as a function of cell concentration for peptide charge $Q = 6$ and two different choices of host cell area A_H as determined in the figures. (a) Both host cells and bacteria have the same cell densities. (b) Host cells have a fixed cell density N_H while bacterial density is varying. Regardless of the choice of cell densities, peptide selectivity is higher for a larger host cell area.

density on peptide therapeutic index defined as MHC/MIC. Fig. 3.12 displays our results for peptide selectivity (MHC/MIC) as a function of cell concentration. We have chosen the density of different target cells in two different ways: (1) density of both host cells and bacteria is the same, (2) density of host cells is fixed and bacterial concentration varies. The second density profile is closer to reality, because it is the concentration of bacteria that changes depending on the degree of infection, and host cells have almost a fixed concentration. As shown in the Fig. 3.12, for both choices of cell densities, peptide selectivity is influenced by cell densities; it decreases as the concentration of cells increases.

In addition, peptide selectivity (MHC/MIC) is higher for a higher host cell area. The reason is that MHC increases by increasing the area of host cells as seen in Fig. 3.11.

To understand the underlying reason for this decreasing behaviour of peptide selectivity by cell density, we repeated our calculations within the simpler Langmuir binding model for the interaction of peptides with the membranes. This model is described in detail in the Appendix B. In the Langmuir binding model, peptide binding is driven with a binding energy w which is dependent on the type of the targets; it is larger on the bacterial membrane than host cells. Analogous to what we did in our full analysis, we calculated the molar ratio of bound peptides to lipids P/L as a function of bulk concentration of peptides for different targets. MHC and MIC were then extracted from the binding curves for varying cell densities. Fig. 3.13 depicts the results for MIC and MHC as a function of cell density. Both MIC and MHC increase as cell density increases. The reasoning is exactly the same as the one given for the results in Fig. 3.11, since this model also considers a fixed number of peptides.

In the end, peptide selectivity (MHC/MIC) was computed for different cell densities. The results are illustrated in Fig. 3.13c. Analogous to our previous approach, the ratio MHC/MIC, which is the measure of peptide selectivity, decreases by increasing the cell density. In order to find out how the choice of peptide threshold concentration P/L^* affects this cell concentration dependence of peptide selectivity, we did the calculations for various choices of P/L^*. More specifically, the peptide threshold concentration on the bacterial membrane P/L^*_B is chosen to be either similar to that on the host cell P/L^*_H or different. As shown in the Fig. 3.13c, regardless of the choice of P/L^*, peptide therapeutic

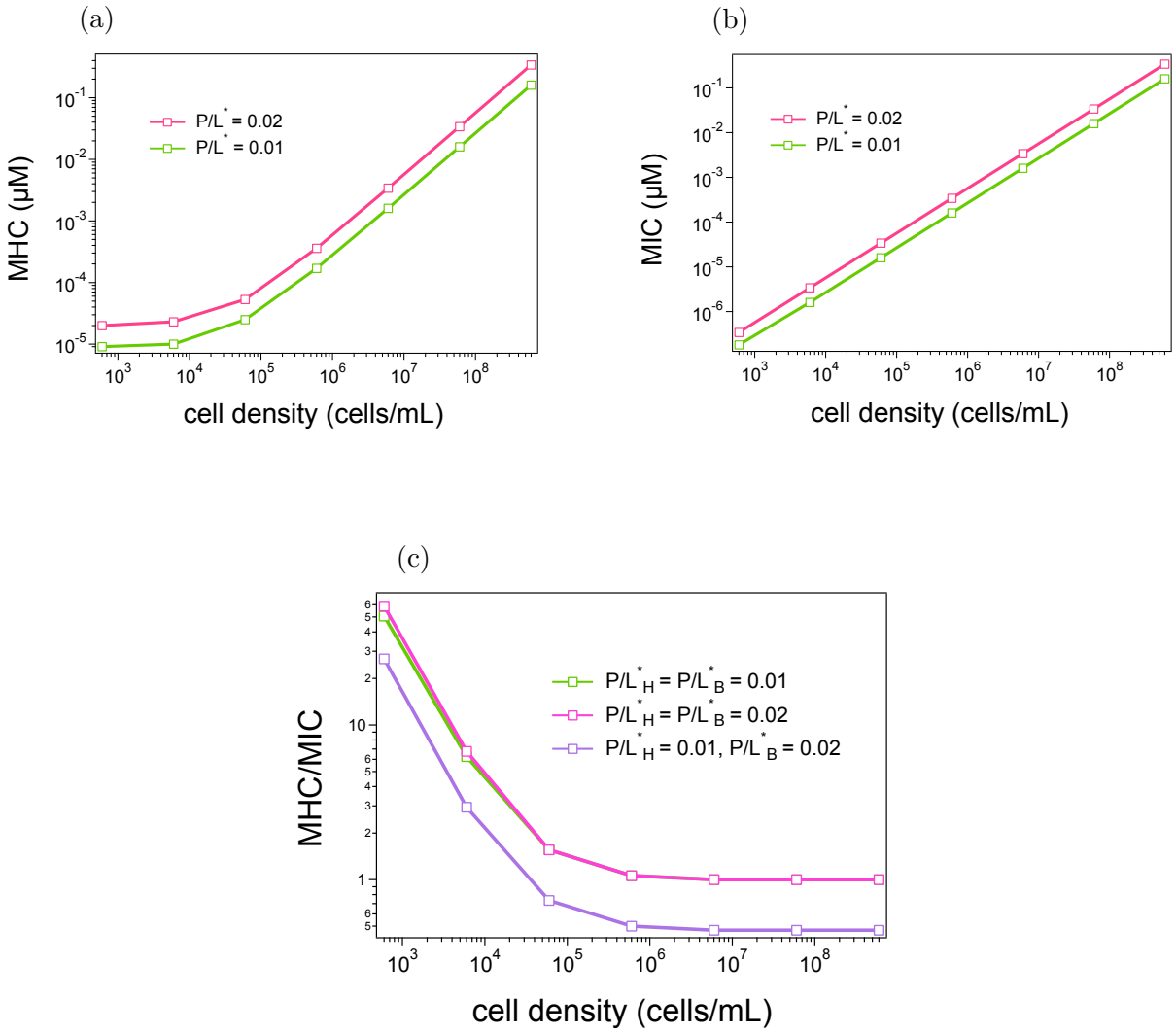

Figure 3.13: Cell concentration dependence of peptide selectivity within the Langmuir binding model: (a) MHC as a function of cell density for different choices of peptide threshold concentration P/L^* as specified in the figure. (b) MIC as a function of cell density for the two different values of P/L^*. (c) MHC/MIC as a function of cell density for different choices of P/L^* on the membranes as specified in the figure.

index (MHC/MIC) decreases as cell density increases. At very high densities, however, it reaches a plateau. The value of this plateau is determined by the choice of P/L^*: For the same threshold concentration on bacterial membrane and host cell, it occurs at 1. Otherwise, it happens at a different value depending on the choice of P/L^*.

In an attempt to understand the reason of the cell concentration dependence of peptide selectivity, we carefully tracked the changes of MIC and MHC by varying the cell density. As shown in the Fig. 3.14, we observed that for a fixed P/L^* the gap between the two P/L curves, which is in fact the difference between MIC and MHC, does not significantly change by changing the cell density. Note that in the figure the log scale falsely gives the appearance of significant change in δ. However, as shown in the Fig 3.15, using a linear scale, it is easily seen that the gap remains the same for various cell concentrations. Thus peptide therapeutic index can be expressed as $\text{MHC/MIC} = (\text{MIC} + \delta)/\text{MIC}$, where δ is fixed and does not depend on the cell density. Therefore, the cell-concentration dependence of the MIC determines the cell concentration dependence of the ratio. As shown in the Fig. 3.13b, MIC increases as cell density increases and as a result the ratio, which measures the peptide selectivity, decreases by increasing the cell density. However, at high cell densities where $\text{MIC} \gg \delta$, the ratio converges to one.

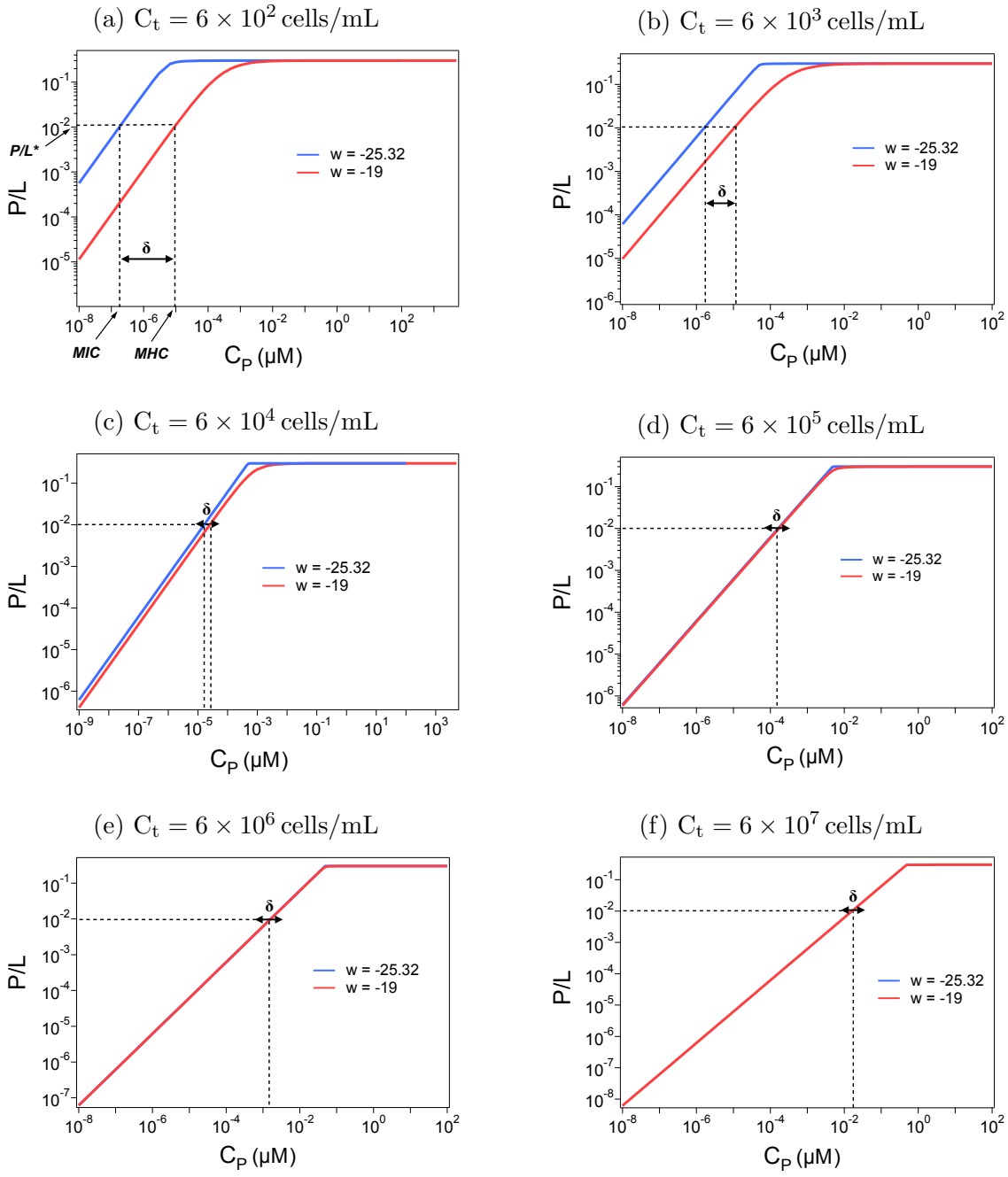

Figure 3.14: P/L as a function of C_p for two different targets: microbe ($w = -25.32$), and host cell ($w = -19$). Peptide binding on two targets is compared for a few choices of cell densities C_t. The gap between the curves δ does not change by increasing the cell density.

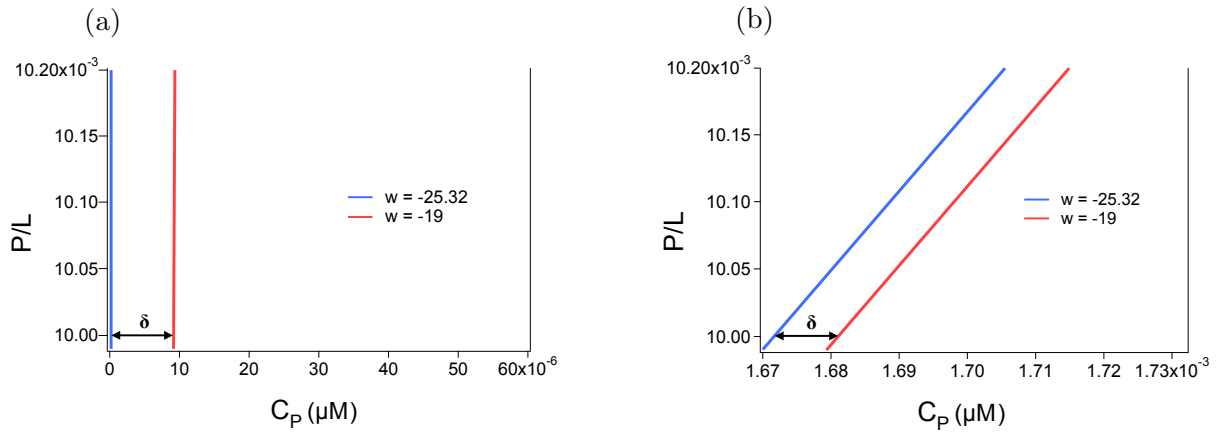

Figure 3.15: (a) Zoom-in plot of Fig. 3.14a for cell density $C_t = 6 \times 10^2$ cells/mL. (b) Zoom-in plot of Fig. 3.14e for cell density $C_t = 6 \times 10^6$ cells/mL. Regardless of the cell density the gap between the two curves is of the order of $10^{-5}\mu M$

Comparison of the results from the single-binding site model with those from the coarse-graining indicated the effect of electrostatic interactions in the cell-concentration dependence of peptide selectivity. Fig. 3.16 depicts MHC/MIC as a function of cell density, computed from two different models. As shown in the figure, except for the very low concentrations, there is good agreement between the results of the two models. Thus, electrostatic interactions do not affect the decreasing behaviour of peptide selectivity by cell density. As seen in the figure, they just cause saturation of the peptide selectivity at low concentrations.

Because of the good agreement between the two models, the reasoning originally proposed for the decreasing trend of peptide selectivity for the Langmuir binding model can be extended to the full analysis.

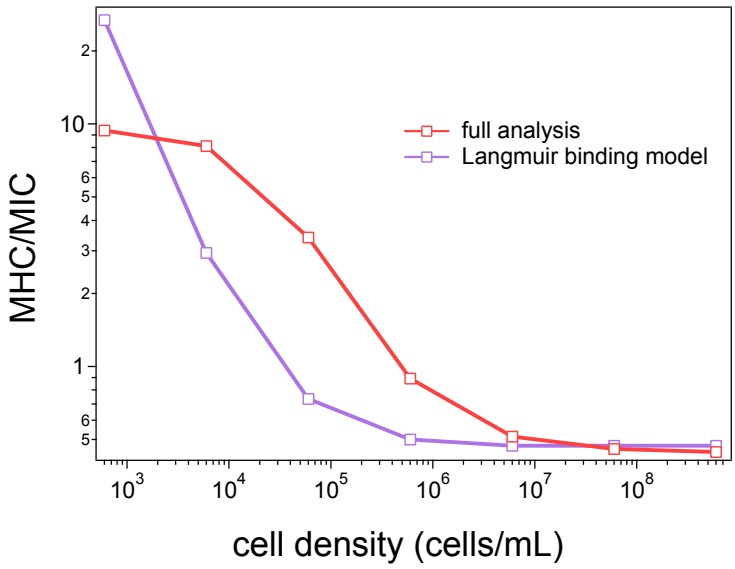

Figure 3.16: MHC/MIC as a function of cell density from two different models: the full analysis based on electrostatic interactions and the Langmuir binding model.

3.5 Summary and Conclusion

To summarize, we presented a physical model for the cell concentration dependence of AMP's activity and cell selectivity. We accomplished this by developing a theoretical model that considers a few pronounced interactions of peptides with lipid bilayers. To investigate the effect of cell density on antimicrobial activity of the peptides, we first calculated the molar ratio of the membrane perturbing peptides, those that are bound to the interface between lipid head group and tail, for various peptide and cell densities. This enabled us to extract the required components to calculate the peptide selectivity: The peptides' minimum hemolytic concentration (MHC) and their minimum concentration that inhibits the growth of bacteria MIC. We showed that both MIC and MHC increase as cell density increases. An increase of MIC means that the peptide activity diminishes as cell density increases. Peptide selectivity was then studied by computing the peptide therapeutic index defined as therapeutic index = MHC/MIC for various cell densities. Our results showed that peptide selectivity is also affected by the cell density; selectivity decreases as cell

density increases.

To discover more about the cell concentration dependence of antimicrobial activity of AMPs, we considered a single-binding site model for the interaction of peptides with the membranes. In this model, many body interactions and peptide-induced mechanical deformation were turned off, and peptides interacted with the membranes only through a fixed binding energy; binding energy was higher on the bacterial membrane than on the host cells. Interestingly, we achieved the same cell concentration dependence for the peptide selectivity using this model. The agreement between the two models led us to the conclusion that the decrease of peptide selectivity with increase of cell density is a general feature of peptide-membrane systems; regardless of the nature of the interactions, the different binding affinity of the peptides for the targets results in a decreasing trend for cell selectivity as a function of cell density.

According to our results, cell selectivity is not an intrinsic feature of antimicrobial peptides as it is attenuated by increasing the cell concentration. Some peptides may even lose their selectivity at very high cell concentrations. Therefore, cell selectivity analysis needs to be done with caution as choosing the wrong host and microbial cell concentrations would result in an inaccurate estimation of the peptide selectivity.

Appendix A

Entropy of the salt ions interacting with a charged surface in a (1:1) electrolyte solution

In an electrolyte solution, the entropy of the salt ions is given as follows

$$F_{ent} = k_B T \Big[\int \Big[n_+ \ln \frac{n_+}{n_0} + n_- \ln \frac{n_-}{n_0} - (n_+ + n_- - 2n_0) \Big] d\mathbf{r} \tag{A.1}$$

where k_B is the Boltzmann constant, T the temperature, $n_+(n_-)$ the density of cations (anions), and n_0 the density of salt ions far from the membrane.

As discussed in chapter 2, the density of the salt ions obeys the Boltzmann distribution

$$n_\pm(\mathbf{r}) = n_0 \exp(\mp e\, \psi(\mathbf{r})/k_B T) \tag{A.2}$$

where e is the electrostatic charge, and $\psi(\mathbf{r})$ the electrostatic potential at position $\mathbf{r}$.

In the case of a weakly charged surface in the solution, the electrostatic potential and consequently the density of the ions is obtained using the Debye-Huckel theory. As

discussed in Sec. 2.2, the electrostatic potential is written as

$$\psi(z) = \frac{\sigma}{\epsilon_0 \epsilon_w \kappa} \exp(-\kappa z) \tag{A.3}$$

where σ is the surface charge density, ϵ_0 the electric permittivity of vacuum, ϵ_w the dielectric constant of the aqueous solution, and κ the inverse of the Debye length. In fact, symmetry of the planar geometry reduces the system to 1-dimension, where the electric potential and the ion densities are only a function of the vertical distance from the surface denoted by z $(n_{\pm}(z), \psi(z))$.

Here, we postpone using the functional form of the potential until the end of the calculation as it would not be clean to substitute it at the beginning. Thus, using the ion densities in Eq. A.2, the entropy in is computed as

$$F_{ent} = A n_0 k_B T \Big[\int_0^{\infty} 2 \frac{e\psi(z)}{k_B T} \sinh(\frac{e\psi(z)}{k_B T}) dz + \int_0^{\infty} \big[-2\cosh(\frac{e\psi(z)}{k_B T}) + 2 \big] dz \Big] \tag{A.4}$$

where A is the surface area.

In the case of a weakly charged surface, $e\psi(z)/k_B T \ll 1$, Eq. A.4 can be further simplified by using the Taylor expansion of the hyperbolic functions. We keep the approximation to the second order of ψ.

$$\begin{aligned} F_{ent} &= A n_0 k_B T \Big[\int_0^{\infty} 2(\frac{e\psi(z)}{k_B T})^2 dz - \int_0^{\infty} (\frac{e\psi(z)}{k_B T})^2 dz \Big] \\ &= A n_0 k_B T \int_0^{\infty} (\frac{e\psi(z)}{k_B T})^2 dz \\ &= A n_0 k_B T \int_{\psi_0}^{0} (\frac{e\psi}{k_B T})^2 (-\frac{1}{\kappa \psi}) d\psi \\ &= \frac{A n_0 e^2 \psi_0^2}{2 k_B T \kappa} = \frac{A\,\sigma^2}{4 \epsilon_w \epsilon_0 \kappa} \end{aligned} \tag{A.5}$$

Note that in the third line, we have changed the variable of integration. In the last line two substitutions have been used: the surface potential $\psi_0 = \sigma/\epsilon_0 \epsilon_w \kappa$ using Eq. A.3 and $\kappa^2 = 8\pi n_0 e^2/(4\pi \epsilon_w \epsilon_0 k_B T)$.

Appendix B

Langmuir binding model

In this model, which is in virtue similar to the Langmuir adsorption model [30], peptide binding is driven by a fixed binding energy indicated as w. There is no interaction between the bound peptides on the membrane. In addition, the total number of peptides in the solution is fixed; there is no peptide reservoir and thus binding on the membranes decreases the concentration of free peptides.

The chemical potential of the peptides bound to the membrane, μ_b, is then written as

$$\mu_b = k_B T \Big[w + \ln \Big(\frac{\sigma A_p}{1 - \sigma A_p} \Big) \Big] \tag{B.1}$$

where k_B is the Boltzmann constant, T the temperature, w the binding energy, σ the area density of the bound peptides, and A_p the area occupied by a bound peptide. The second term describes the translational entropy of the bound peptides, which is obtained by considering a 2D lattice model; the membrane is assumed to be like a 2D lattice with the total number of peptide binding sites defined as $S = A/A_p$, where A is the membrane area. Indeed, σA_p gives the area density of the filled binding sites.

In this model, we consider a dilute solution of peptides and cells. Thus, there is no interaction between the free peptides or between the cells. Note that the electrostatic energy of each free peptide is subsumed in its binding energy. Thus, we have only translational

entropy associated with the free peptides and their chemical potential has the form

$$\mu_f = k_B T \ln[(C_p - C_t \sigma A) v_p] \tag{B.2}$$

where C_p is the total concentration of the peptides in the solution, C_t the concentration of the target cells, A the area of each cell, and v_p the volume of a free peptide.

Balancing the two chemical potentials, we obtain a Langmuir-like binding equation

$$\sigma A_p = \frac{(C_p - C_t A \sigma) K}{1 + (C_p - C_t A \sigma) K} \tag{B.3}$$

with K the binding constant defined as $K = v_p \exp(-w/k_B T)$. Here, the concentration of free peptides in bulk, which is given inside the parentheses of the equation, is indeed dependent on the number of bound peptides because the total number of peptides is conserved.

In order to find σ as a function of C_p, we should solve the Eq. B.3 for σ which results in the following equation

$$-C_t\, A\, K\, A_p \sigma^2 + \left(A_p + K\, A_p\, C_p + C_t\, A\, K\right) \sigma - C_p\, K = 0 \tag{B.4}$$

It is worth noting that there are two solutions for Eq. B.4, however, our desired solution is the one that fulfils $\sigma \leqq 1/A_p$, *i.e.,* σ can not be larger than the area density of the peptide binding sites on the membrane. To rewrite the Eq. B.4 as a function of ratio of bound peptides to lipids P/L, we just need to make the following conversion everywhere $\sigma = (P/L)\, 1/a_l$, where a_l is the lipid head group area.

In this model, w is the only parameter which depends on the type of the target. Peptides have a higher binding energy w on the bacterial membrane than on host cells because of stronger electrostatic interactions with the former. We have obtained w for different targets by fitting the P/L from Eq. B.4 to the binding isotherms we obtained from the coarse-grained approach. The result is as follows; for the bacterial membrane $w = -25.32$, and for the host cell $w = -19$.

Appendix C

The MATLAB Code used in the project

```
clc
clear all
global Q al alph kapain Cp ap apef lb rp

Eps = 8.85e-12;
T = 300;
Kb = 1.38*1e-23;
Dw = 80;
NA = 6.023*1e+23;
e = 1.6e-19;
lb = e^2*1e+10/(4*pi*Eps*Dw*Kb*T);
kapain = 10;  %Angstrom
C_0 = 1/(kapain^2 *8*pi*lb);

%Melittin
```

```
al = 71; %74, 65
ap = 162 %246, 314
apef = ap;  %symmetric binding
%apef = ap/2 for asymmetric binding

SM = 1/ap;

alph = 0.3; %0.05
Q = 6;

rp = sqrt(ap/pi);
lambda = al/(2*pi*lb*alph);
As = pi*(rp+lambda)^2;

%Host
%single target
%c_p = [ 0.0001 0.00012 0.0002 0.0003 0.0005 0.0007 0.001 0.005
    0.01 0.03 0.05 0.1 0.3 0.7 0.9 1 3 4 5 7 9 10 15 20 30 40 50
    60 70 80 90 100 200 300 400 500 600 700 800 900 1000 2000
    3000]

%N_h = 6e2 - 6e5
%c_mic = [ 1e-4 1.2e-4 2e-4 3e-4 5e-4 7e-4 1e-3 2e-3 3e-3 4e-3 5e
    -3 7e-3 0.01 0.03 0.05 0.1 0.3 0.7 0.9 1 3 4 5 7 9 10 15 20 30
     40 50 60 70 80 90 100 200 300 400 500 600 700 800 900 1000
    2000 3000]

%N_h = 6e6
%c_mic = [ 1e-4 2e-4 3e-4 5e-4 7e-4 1e-3 2e-3 3e-3 4e-3 5e-3 7e-3
     0.01 0.014 0.017 0.023 0.026 0.03 0.04 0.05 0.1 0.3 0.7 0.9 1
```

```
    3 4 5 7 9 10 15 20 30 40 50 60 70 80 90 100 200 300 400 500
    600 700 800 900 1000 2000 3000]

%N_h = 6e7
%c_mic = [ 7e-4 1e-3 2e-3 3e-3 4e-3 5e-3 7e-3 0.01 0.014 0.017
    0.023 0.026 0.03 0.04 0.05 0.07 0.1 0.13 0.17 0.2 0.32 0.35
    0.4 0.5 0.6 0.7 0.9 1 3 4 5 7 9 10 15 20 30 40 50 60 70 80 90
    100 200 300 400 500 600 700 800 900 1000 2000 3000]

%N_h = 6e8
%c_mic = [0.017 0.023 0.026 0.03 0.04 0.05 0.07 0.1 0.13 0.17 0.2
     0.32 0.35 0.4 0.5 0.6 0.7 0.9 1 1.3 1.5 2 2.5 2.6 3.7 3.8 4 5
     7 9 10 15 20 30 40 50 60 70 80 90 100 200 300 400 500 600 700
     800 900 1000 2000 3000]

%N_h = 6e9
%c_mic = [0.1 0.13 0.17 0.2 0.32 0.35 0.4 0.5 0.6 0.7 0.9 1 1.3
    1.5 2 2.5 2.6 3.7 3.8 4 5 7 9 10 15 20 30 35 37 40 43 45.8 46
    50 60 70 80 90 100 200 300 400 500 600 700 800 900 1000 2000
    3000]



%Bacteria
%single target
%c_mic = [1e-6 3e-6 6.7e-6  9.854e-6 1.2e-5  2.34e-5 3.5e-5  5e-5
     8.876e-5  1e-4  3.788e-4  6e-4 9e-4 1e-3 3e-3 9e-3 2e-2 4e-2
    6e-2 0.1 0.3 0.5 0.7 1 3 6  8 10 20 30 50 60 80 100 ];

%N_b = 6e2, 6e3, 6e4
c_mic = [1e-6 3e-6 6.7e-6  9.854e-6 1.2e-5  2.34e-5 3.5e-5  5e-5
```

```
    8.876e-5  1e-4  3.788e-4  6e-4 9.9101e-4  3.79094e-3  9.82101
   e-3  2.05505e-2  4.5557e-2  6.25669e-2  9.73273e-2
   0.143712  0.203657  0.279167  0.372308  0.485207
   0.620045  0.779055  0.964523  1.17878  1.4242  1.70321
   2.01826  2.37187  2.76657  3.20495  3.6  6 7 8 10 20 30 40
    50 60 80 90 100 ];

%N_b = 6e5
%c_mic = [ 4e-6 5e-6 8e-6 1.2e-5  2.34e-5 3.5e-5  5e-5 6e-5 8.876
   e-5  1.3e-4  2e-4 3.788e-4 5e-4 6e-4 9.9101e-4 1.3e-3 1.5e-3 2
   e-3 3e-3  3.79e-3  9.82101e-3  2.05505e-2  4.5557e-2
   6.25669e-2  9.73273e-2  0.143712  0.203657  0.2  0.372308
    0.485207  0.620045  0.779055  0.964523  1.17878
   1.4242  1.70321  2.01826  2.37187  2.76657  3.20495
   3.68961  4.22322  4.80845  5.44803  6.14471  6.90127
   7.72052  8.60531  9.55852  10.583  15.4534 20 30 40 50 60
   70 80 90 100 ];

%N_b = 6e6
%c_mic = [2e-5 5e-5 8.876e-5 1.3e-4 2e-4 3.788e-4 6.2e-4 8e-4
   9.9101e-4 1.3e-3 2.2e-3 3.79094e-3 5e-3 6e-3 7e-3 8e-3 9.82101
   e-3 1e-2 2e-2  3e-2  4.5557e-2  6.25669e-2  9.73273e-2
   0.143712  0.203657  0.279167  0.372308  0.485207
   0.620045  0.779055  0.964523  1.17878  1.4242  1.70321
   2.01826  2.37187  2.76657  3.20495  3.68961  4.22322
   4.80845  5.44803  6.14471  6.90127  7.72052  8.60531
   9.55852  10.583  15.4534 20 30 40 50 60 70 80 90 100 ];

%N_b = 6e7
%c_mic = [1e-4 1.3e-4  2e-4 3e-4 8e-4 1e-3 2e-3 3e-3 5e-3 7e-3 8e
```

```
    -3 1e-2 1.3e-2 2e-2 3e-2 4.5e-2 6.25669e-2 7.1e-2 8e-2 9
    e-2 0.1 0.12 0.143712 0.203657 0.279167 0.372308
    0.485207 0.620045 0.779055 0.964523 1.17878 1.4242
      1.70321 2.01826 2.37187 2.76657 3.20495 3.68961
    4.22322 4.80845 5.44803 6.14471 6.90127 7.72052
    8.60531 9.55852 10.583 15.4534 20 30 40 50 60 70 80 90
    100 ];

%N_b = 6e8
%c_mic = [2e-3 3e-3 5e-3 7e-3 8e-3 1e-2 1.5e-2 2e-2 4e-2 5.2e-2
    6.1e-2 7e-2 9.7e-2 0.143712 0.203657 0.279167 0.372308
      0.485207 0.55 0.620045 0.65 0.779055 0.964523 1.17878
      1.4242 1.70321 2.01826 2.37187 2.76657 3.20495
    3.68961 4.22322 4.80845 5.44803 6.1 6.9 7.72052
    8.60531 9.55852 10.583 15.4534 20 30 40 50 60 70 80 90
    100 ];

%N_b = 6e9
%c_mic = [ 2e-2 3e-2 4e-2 7e-2 0.143 0.2 0.27 0.37 0.48 0.6 0.7
    1 1.3 1.7 2.1 2.5 2.7 3 3.9 5.2 5.8 6.8 7.6 8 9 10.583
    15.4534 20 30 40 50 60 70 80 90 100];

%no demixing
%options = optimset('MaxFunEvals',1e4, 'MaxIter', 1e6, 'TolX', 1e
    -12, 'TolFun', 1e-12);

% lipid demixing
options = optimset('Display','iter','Algorithm','interior-point',
    'InitBarrierParam',0.1, 'TolCon', 1e-6,'MaxFunEvals',5e3, '
    MaxIter', 1e6, 'TolX', 1e-10, 'TolFun', 1e-10);
```

```
%x0 = [1e-6; 1e-9]; %for alph = 0.05 and Epsilon = -14

x0 = [2e-6; 6e-7; 0.5; 0.3] %for N_b = 6e2-6e5
%x0 = [1e-6; 6e-8; 0.5; 0.3] %6e6
%x0 = [7e-7; 7e-8; 0.5; 0.3]; %6e7
%x0 = [7e-7; 8e-9; 0.5; 0.3] %6e8
%x0 = [8e-11; 5e-12; 0.5; 0.3] %6e9


L = length(c_mic);

for n = 1:L
    Cp = c_mic(n)*(1e-6)*NA*(1e-27);  % bulk peptide concentration
        (1/Angs^3)

    %no lipid demixing
    %[x, fval] = fminsearch(@(x)lipid(x),x0,options) %no lipid
        demixing

   % lipid demixing
   [x, fval, exitflag] = fmincon(@(x)energy(x),x0,[(As-apef) As 0
       0],[1],[],[],[0;0;0;0],[SM;SM;1;1],'constraint',options)

    %x0 = [x(1),x(2),x(3),x(4)];
    %x0=[x(1),x(2)];

   P_L(n,1) = c_mic(n);
   P_L(n,2) = x(1)*al
end
```

```
dlmwrite('P_L.txt', P_L, 'delimiter', '\t' , 'precision', 6)

X = c_mic;
plot(X,P_L(:,2))
ylabel('P_L','fontsize',12,'fontweight','b')
xlabel('cp','fontsize',12,'fontweight','b')
```

C.1 The function to calculate the free energy of the peptide-membrane system

```
function G = lipid(x)
global Q al alph ap Cp apef

Eps = 8.85e-12;
T = 300;
Kb = 1.38*1e-23;
Dw = 80;
NA = 6.023*1e+23;
e = 1.6e-19;
lb = e^2*1e+10/(4*pi*Eps*Dw*Kb*T);
kapain = 10;  %Angstrom
C_0 = 1/(kapain^2 *8*pi*lb);

Ac = 6e8;     %Bacterium surface area in aangstrom^2
Ah = 1e10;    %Host cell surface area in aangstrom^2
ap = 162; %246, 314
apef = ap;  %symmetric binding
%apef = ap/2 for asymmetric binding
al = 71; %74, 65
alph = 0.3; %0.05
Q = 6;

%Magainin
%vp = 2512; %V=314*8 A^3

%Melittin
vp = 33^3;
```

```
V = 1e27; % total volume in Angstrom^3

Ct = 6e4*1e-24; %cell density(cells/(A^3)
A = 2*Ac; %symmetric binding
%A = Ac    %Asymmetric binding

KA = 0.578;   %KbT/A^2
SM = 1/ap ;

%FE = (x(1)*WSIND(x)+x(2)*WSSND(x));   %without lipid demixing
FE = x(1)*WSI(x(1),x(2),x(3))+x(2)*WSS(x(1),x(2),x(4));   %with
    lipid demixing

ME = (1/2)*KA*(x(1)*apef)^2;

% with peptide reservoir
%EntG = x(1)*log(x(1)*ap/(cp*vp)) + (SM-x(1)-x(2))*log(1-((x(1)+x
    (2))/SM)) + x(2)*log(x(2)*ap/(cp*vp));

% without peptide reservoir
Ent_b = x(1)*log(x(1)*ap) + (SM-x(1)-x(2))*log(1-((x(1)+x(2))/SM)
    ) + x(2)*log(x(2)*ap);
Ent_f = (1/(V*Ct*A))*( V*(Cp-Ct*A*(x(1)+x(2)))*log((Cp-Ct*A*(x(1)
    +x(2)))*vp) - (Cp*V-Ct*V*A*(x(1)+x(2))) - (Cp*V*log(Cp*vp)-Cp*
    V));


    ;

EntC = Ent_b + Ent_f;
```

```
%F_reference
S_0 = -alph/al;
Ps = 2*asinh(2*pi*S_0*lb*kapain);
Fm = S_0*Ps - (cosh(Ps/2)-1)/(kapain*pi*lb);
Entm = (alph*log(alph)+(1-alph)*log(1-alph))/al;

%magainin
%E_coil = [0.1755    1.1663    2.7428    4.7889    7.2350
    10.0339    13.1510    16.5596    20.2384    24.1697];
% melittin
E_coil = [0.0352    0.7136    1.8818    3.4487    5.3573
    7.5683    10.0524    12.7872    15.7544    18.9392];
Fp = (x(1)+x(2))*E_coil(Q);

F_ref = Fp + Fm + Entm;

G = FE + ME + EntC - F_ref;
```

C.2 The function to calculate the WSC free energy

```
function FWSI = WSI(J,S,K) %membrane-inserted peptides

global Q alph al apef ap

Eps = 8.85e-12;
T = 300;
Kb = 1.38*1e-23;
Dw = 80;
NA = 6.023*1e+23;
e = 1.6e-19;
lb = e^2*1e+10/(4*pi*Eps*Dw*Kb*T);
kapain = 10;  %Angstrom
C_0 = 1/(kapain^2 *8*pi*lb);
rp = sqrt(ap/pi);

x(1) = J;
x(2) = S;
alfp = K;

Aws = (1+x(1)*apef)/(x(1)+x(2));
lambda = al/(2*pi*lb*alph);
As = pi*(rp+lambda)^2;

%Zone1
Sigp = Q/As - alfp*(As-ap)/(al*As);
psip = 2*asinh(2*pi*Sigp*lb*kapain);
F1 = Sigp*psip - (cosh(psip/2)-1)/(kapain*pi*lb);
Ent1 = (alfp*log(alfp)+(1-alfp)*log(1-alfp))/al;
```

```
%zone2
alf = (alph*(Aws-ap)-alfp*(As-ap))/(Aws-As);
sig = -alf/al;
psi = 2*asinh(2*pi*sig*lb*kapain);
F2 = sig*psi - (cosh(psi/2)-1)/(kapain*pi*lb);
Ent2 = (alf*log(alf)+(1-alf)*log(1-alf))/al;

eh = -14; %hydrophobic energy

FWSI = As*F1 + (Aws-As)*F2 + Ent1*(As-ap) + Ent2*(Aws-As) + eh;



function FWSS = WSS(D,B,N) %surface-adsorbed peptides

global Q As alph al apef ap

Eps = 8.85e-12;
T = 300;
Kb = 1.38*1e-23;
Dw = 80;
NA = 6.023*1e+23;
e = 1.6e-19;
lb = e^2*1e+10/(4*pi*Eps*Dw*Kb*T);
kapain = 10;  %Angstrom
C_0 = 1/(kapain^2 *8*pi*lb);
rp = sqrt(ap/pi);

x(1) = D;
x(2) = B;
```

```
alfp = N;

Aws = (1+x(1)*apef)/(x(1)+x(2));
lambda = al/(2*pi*lb*alph);
As = pi*(rp+lambda)^2;

%Zone1
Sigp = Q/As - alfp/al;
psip = 2*asinh(2*pi*Sigp*lb*kapain);
F1 = Sigp*psip - (cosh(psip/2)-1)/(kapain*pi*lb);
Ent1 = (alfp*log(alfp)+(1-alfp)*log(1-alfp))/al;

%zone2
alf = (alph*Aws-alfp*As)/(Aws-As);
sig = -alf/al;
psi = 2*asinh(2*pi*sig*lb*kapain);
F2 = sig*psi - (cosh(psi/2)-1)/(kapain*pi*lb);
Ent2 = (alf*log(alf)+(1-alf)*log(1-alf))/al;

FWSS = As*F1 + (Aws-As)*F2 + Ent1*As + Ent2*(Aws-As);
```

References

[1] Sattar Taheri-Araghi. *Membrane-Disrupting Activity of Antimicrobial Peptides and the Electrostatic Bending of Membranes*. Ph. d. thesis, University of Waterloo, 2010.

[2] Andrea Giuliani, Giovanna Pirri, and Silvia Fabiole Nicoletto. Antimicrobial peptides: an overview of a promising class of therapeutics. *Central European Journal of Biology*, 2(1):1–33, March 2007.

[3] Tomas Ganz. The role of antimicrobial peptides in innate immunity. *Integrative and comparative biology*, 43(2):300–4, April 2003.

[4] Mukesh Pasupuleti, Artur Schmidtchen, and Martin Malmsten. Antimicrobial peptides: key components of the innate immune system. *Critical reviews in biotechnology*, 32(2):143–71, June 2012.

[5] Ziqing Jiang, Adriana I Vasil, John D Hale, Robert E W Hancock, Michael L Vasil, and Robert S Hodges. Effects of net charge and the number of positively charged residues on the biological activity of amphipathic alpha-helical cationic antimicrobial peptides. *Biopolymers*, 90(3):369–83, January 2008.

[6] Margitta Dathe, Heike Nikolenko, Jana Meyer, Michael Beyermann, and Michael Bienert. Optimization of the antimicrobial activity of magainin peptides by modification of charge. *FEBS Letters*, 501(2-3):146–150, July 2001.

[7] W. Lee Maloy and U. Parsad Kari. Structure-activity studies on magainins and other host defense peptides. *Biopolymers*, 37(2):105–22, January 1995.

[8] Katsumi Matsuzaki. Control of cell selectivity of antimicrobial peptides. *Biochimica et biophysica acta*, 1788(8):1687–92, August 2009.

[9] Sattar Taheri-Araghi and Bae-Yeun Ha. Cationic antimicrobial peptides: a physical basis for their selective membrane-disrupting activity. *Soft Matter*, 6(9):1933, 2010.

[10] Michael Zasloff. Antimicrobial peptides of multicellular organisms. *Nature*, 415:389–395, 2002.

[11] Robert E. W. Hancock and Monisha G. Scott. The role of antimicrobial peptides in animal defenses. *Proceedings of the National Academy of Sciences of the United States of America*, 97(16):8856–61, August 2000.

[12] Katsumi Matsuzaki. Why and how are peptide-lipid interactions utilized for self-defense? Magainins and tachyplesins as archetypes. *Biochimica et biophysica acta*, 1462(1-2):1–10, December 1999.

[13] Bruce Alberts, Alexander Johnson, Julian Lewis, Martin Raff, Keith Roberts, and Peter Walter. *Molecular Biology of the Cell*. Garland Science, 2002.

[14] Geoffrey M. Cooper and Robert E. Hausmn. *The cell: a molecular approach*. Sinauer, 3 edition, 2004.

[15] Sylvie E. Blondelle and Richard A. Houghten. Hemolytic and antimicrobial activities of the twenty-four individual omission analogues of melittin. *Biochemistry*, 30(19):4671–8, May 1991.

[16] Narasimhaiah Sitaram and Ramakrishnan Nagaraj. Interaction of antimicrobial peptides with biological and model membranes: structural and charge requirements for activity. *Biochimica et biophysica acta*, 1462(1-2):29–54, December 1999.

[17] Kim A Brogden. Antimicrobial peptides: pore formers or metabolic inhibitors in bacteria? *Microbiology*, 3:238–250, 2005.

[18] Yechiel Shai. Mechanism of the binding, insertion and destabilization of phospholipid bilayer membranes by alpha-helical antimicrobial and cell non-selective membranelytic peptides. *Biochimica et biophysica acta*, 1462(1-2):55–70, December 1999.

[19] Gustavo Fuertes, Diana Giménez, Santi Esteban-Martin, Anaj Garcia-Sáez, Orlando Sánchez, and Jesús Salgado. Role of membrane lipids for the activity of pore forming peptides and proteins. *Advances in experimental medicine and biology*, 677:31–55, January 2010.

[20] Huey W Huang. Molecular mechanism of antimicrobial peptides: the origin of cooperativity. *Biochimica et biophysica acta*, 1758(9):1292–302, September 2006.

[21] Ming-Tao Lee, Fang-Yu Chen, and Huey W Huang. Energetics of pore formation induced by membrane active peptides. *Biochemistry*, 43(12):3590–9, March 2004.

[22] Ming-Tao Lee, Wei-Chin Hung, Fang-Yu Chen, and Huey W Huang. Many-body effect of antimicrobial peptides: on the correlation between lipid's spontaneous curvature and pore formation. *Biophysical journal*, 89(6):4006–16, December 2005.

[23] Fang-Yu Chen, Ming-Tao Lee, and Huey W Huang. Evidence for membrane thinning effect as the mechanism for peptide-induced pore formation. *Biophysical journal*, 84(6):3751–8, June 2003.

[24] Adam a. Strömstedt, Lovisa Ringstad, Artur Schmidtchen, and Martin Malmsten. Interaction between amphiphilic peptides and phospholipid membranes. *Current Opinion in Colloid & Interface Science*, 15(6):467–478, December 2010.

[25] Lin Yang, Thad A. Harroun, Thomas M. Weiss, Lai Ding, and Huang W. Huang. Barrel-stave model or toroidal model? A case study on melittin pores. *Biophysical journal*, 81(3):1475–85, October 2001.

[26] Katsumi Matsuzaki, Ken-ichi Sugishita, Noriko Ishibe, Mayu Ueha, Saori Nakata, Koichiro Miyajima, and Richard M. Epand. Relationship of membrane curvature to the formation of pores by magainin 2. *Biochemistry*, 37(34):11856–63, August 1998.

[27] David Boal. *Mechanics of the Cell*. Cambridge University Press, 2002.

[28] Hiroshi Nikaido. Molecular basis of bacterial outer membrane permeability revisited. *Microbiology and Molecular Biology Reviews*, 67(4):593–656, 2003.

[29] Jonathan Widom and Robert L. Baldwin. Cation-induced toroidal condensation of DNA: studies with Co3+(NH3)6. pages 431–453, 1980.

[30] Ken A. Dill and Bromberg Sarina. *Molecular driving forces: statistical thermodynamics in chemistry and biology*. Garland Science, 2002.

[31] Thomas Heimburg. *Thermal biophysics of membranes*. WILEY-VCH, 2007.

[32] Geert van den Bogaart, Jeanette Velásquez Guzmán, Jacek T Mika, and Bert Poolman. On the mechanism of pore formation by melittin. *The Journal of biological chemistry*, 283(49):33854–7, December 2008.

[33] Manuel N Melo, Rafael Ferre, and Miguel a R B Castanho. Antimicrobial peptides: linking partition, activity and high membrane-bound concentrations. *Nature reviews. Microbiology*, 7(3):245–50, March 2009.

[34] Torsten Wieprecht, Michael Beyermann, and Joachim Seelig. Thermodynamics of the coil-alpha-helix transition of amphipathic peptides in a membrane environment: the role of vesicle curvature. *Biophysical chemistry*, 96(2-3):191–201, May 2002.

[35] Gabriela Klocek, Therese Schulthess, Yechiel Shai, and Joachim Seelig. Thermodynamics of melittin binding to lipid bilayers. Aggregation and pore formation. *Biochemistry*, 48(12):2586–96, March 2009.

[36] Thomas Heimburg, Brigitta Angerstein, and Derek Marsh. Binding of peripheral proteins to mixed lipid membranes: effect of lipid demixing upon binding. *Biophysical journal*, 76(5):2575–86, May 1999.

[37] Joachim Seelig, Simon Nebel, Peter Ganz, and Christian Bruns. Electrostatic and nonpolar peptide-membrane interactions. Lipid binding and functional properties of somatostatin analogues of charge z)+1 to z)+3. *Biochemistry*, 32:9714–9721, 1993.

[38] Torsten Wieprecht, Michael Beyermann, and Joachim Seelig. Binding of antibacterial magainin peptides to electrically neutral membranes: thermodynamics and structure. *Biochemistry*, 38(32):10377–87, August 1999.

[39] Sylvio May, Daniel Harries, and Avinoam Ben-shaul. Lipid demixing and protein-protein interactions in the adsorption of charged proteins on mixed membranes. 79(July):1747–1760, 2000.

[40] Esov S. Velazquez and Lesser Blum. Electrolytes confined to a plane in the Debye-Huckel theory. *Physica A: Statistical Mechanics and its Applications*, pages 453–460, 1997.

[41] Andrey V. Dobrynin and Michael Rubinstein. Theory of polyelectrolytes in solutions and at surfaces. *Progress in Polymer Science*, 30(11):1049–1118, November 2005.

[42] Pierre-Gilles de Gennes. *Scaling concepts in polymer physics*. Cornell University Press, 1979.

[43] A. Katchalsky, S. Lifson, and J. Mazur. The electrostatic free energy of polyelectrolyte solutions. I. Randomly kinked macromolecules. *Journal of Polymer Science*, 11(5):409–423, November 1953.

[44] Stuart McLaughlin. The electrostatic properties of membranes. *Annual review of biophysics and biophysical chemistry*, 18:113–36, January 1989.

[45] Terrell L. Hill. *An introduction to statistical thermodynamics*. Dover Publications, Inc., 1986.

[46] Huey Huang, Fang-Yu Chen, and Ming-Tao Lee. Molecular Mechanism of Peptide-Induced Pores in Membranes. *Physical Review Letters*, 92(19):198304, May 2004.

[47] William T Heller, Ke He, Steve J Ludtke, Thad A Harroun, and Huey W Huang. Effect of Changing the Size of Lipid Headgroup into Membranes Peptide Insertion. 73(July):239–244, 1997.

[48] Ming-Tao Lee, Wei-Chin Hung, Fang-Yu Chen, and Huey W Huang. Mechanism and kinetics of pore formation in membranes by water-soluble amphipathic peptides. *Proceedings of the National Academy of Sciences of the United States of America*, 105(13):5087–92, April 2008.

[49] Torsten Wieprecht, Ognjan Apostolov, Michael Beyermann, and Joachim Seelig. Membrane binding and pore formation of the antibacterial peptide PGLa: thermodynamic and mechanistic aspects. *Biochemistry*, 39(2):442–52, January 2000.